Agricultural and Forest Meteorology 187 (2014) 22–35

Contents lists available at ScienceDirect

Agricultural and Forest Meteorology

journal homepage: www.elsevier.com/locate/agrformet

Simultaneous leaf- and ecosystem-level fluxes of volatile organic compounds from a poplar-based SRC plantation

Federico Brilli[a,b,*], Beniamino Gioli[c], Donatella Zona[d], Emanuele Pallozzi[e], Terenzio Zenone[a], Gerardo Fratini[f], Carlo Calfapietra[e], Francesco Loreto[g], Ivan A. Janssens[a], Reinhart Ceulemans[a]

[a] Department of Biology, University of Antwerp, Research group of Plant and Vegetation Ecology, Research Group of Plant and Vegetation Ecology, Universiteitsplein 1, B-2610 Wilrijk, Belgium
[b] National Research Council, Institute of Agro-Environmental and Forest Biology (IBAF-CNR), Via Salaria Km 29,300 – 00016 Monterotondo Scalo,, Roma, Italy
[c] National Research Council, Biometeorology Institute (IBIMET-CNR), Via G. Caproni 8-50145, Firenze, Italy
[d] Department of Animal and Plant Sciences, University of Sheffield, Western Bank, S10 2TN Sheffield, UK
[e] National Research Council, Institute of Agro-Environmental and Forest Biology (IBAF-CNR), Via Marconi 2 – 05010 Porano, Terni, Italy
[f] LI-COR Biosciences GmbH, Siemensstr. 25a-61352, Bad Homburg, Germany
[g] National Research Council, Department of Biology, Agriculture and Food Sciences (CNR-DISBA), piazzale Aldo Moro 7-00185 Roma, Italy

ARTICLE INFO

Article history:
Received 26 July 2013
Received in revised form 6 November 2013
Accepted 18 November 2013

Keywords:
VOC
PTR–TOF–MS
Fluxes
Poplar
Eddy covariance

ABSTRACT

Emission of carbon from ecosystems in the form of volatile organic compounds (VOC) represents a minor component flux in the global carbon cycle that has a large impact on ground-level ozone, particle and aerosol formation and thus on air chemistry and quality. This study reports exchanges of CO_2 and VOC between a poplar-based short rotation coppice (SRC) plantation and the atmosphere, measured simultaneously at two spatial scale, one at stand level and another at leaf level. The first technique combined Proton Transfer Reaction "Time-of-Flight" mass spectrometry (PTR–TOF–MS) with the eddy covariance method, to measure fluxes of a multitude of VOC. Abundant fluxes of isoprene, methanol and, to a lesser extent, fluxes of other oxygenated VOC such as formaldehyde, isoprene oxidation products (methyl vinyl ketone and methacrolein), methyl ethyl ketone, acetaldehyde, acetone and acetic acid, were measured. Under optimal environmental conditions, isoprene flux was mostly controlled by temperature and light. Differently, methanol flux underwent a combined enzymatic and stomatal control, together involving environmental drivers such as vapour pressure deficit (VPD), temperature and light intensity. Moreover fair weather condition favoured ozone deposition to the poplar plantation.

The second technique involved trapping the VOCs emitted from leaves followed by gas chromatography-mass spectrometry (GC–MS) analysis. These leaf-level measurements showed that emission of isoprene in adult leaves and of monoterpenes in juvenile leaves are widespread across poplar genotypes. Detection of isoprene oxidation products (i_{ox}) emission with leaf-level measurements confirmed that a fraction of isoprene may be already oxidized within leaves, possibly when isoprene copes with foliar reactive oxygen species (ROS) formed during warm and sunny days.

1. Introduction

Bioenergy is gaining considerable attention among public and industrial investment (EU, 2009; U.S., 2011) and will inevitably imply a future expansion of landmass available for biomass-based energy sources over the next 20 years (Fisher et al., 2010; Özdemir et al., 2009). Producing bioenergy from woody biomass is indeed beneficial on marginal lands where the potential for food production is minor and tree cultivation can become a competitive land-use (IPC, 2013).

Poplars (*Populus spp.*) are particularly suitable to provide a constant supply of woody biomass since they are fast growing trees (Weih, 2004) with high rates of photosynthesis (Vitousek, 1991). Therefore, poplars have the potential to mitigate rising atmospheric CO_2 concentration through their high uptake of carbon and production of considerable amounts of biomass, especially when grown as short-rotation coppice (SRC) (Calfapietra et al., 2010). However,

* Corresponding author. Tel.: +39 (0)6 90672525; fax: +39 (0)6 9064492.
E-mail address: federico.brilli@ibaf.cnr.it (F. Brilli).

0168-1923
http://dx.doi.org/10.1016/j.agrformet.2013.11.006

a future intensive use of SRC might impact on land use change (Fargione et al., 2008) and on the greenhouse gas emissions to the atmosphere (Searchinger et al., 2008). In addition, re-emission of small amounts of carbon in the atmosphere in the form of reactive volatile organic compounds (VOC) (Guenther et al., 1993) coupled with elevated concentrations of nitrogen oxides (NO_x) and favorable conditions of sunlight and temperature, may promote ground-level ozone formation (Ashworth et al., 2013) and enhance the formation of aerosols (Kulmala et al., 2001).

Isoprene is among the main VOC released in the atmosphere by many plants. *Populus spp.* are known to be among the strongest isoprene-emitting plant species (Guidolotti et al., 2011). Generally, isoprene-emitting plants do not emit substantial amounts of other isoprenoids (Kesselmeier and Staudt, 1999), but low emissions of monoterpenes have been reported in young *Populus tremula* (Hakola et al., 1998) and *Populus x euroamericana* leaves (Brilli et al., 2009), as well as in leaves attacked by herbivorous insects (Brilli et al., 2009). Isoprene and monoterpenes (collectively called volatile isoprenoids) are produced directly from photosynthates (Loreto and Sharkey, 1990; Loreto and Schnitzler, 2010) by isoprene synthase (IspS) and monoterpenes synthases (TPS) enzymes, respectively. The two classes of enzymes respond exponentially to rising temperature having optimum activities between 40 and 45 °C (Monson et al., 1992; Sharkey and Yeh, 2001; Staudt and Lhoutellier, 2011).

Within leaves, isoprene can act as an antioxidant and protect plants against the excessive production of reactive oxygen species (ROS), such as singlet oxygen ($^1O_2$), superoxide ($O_2^{\bullet -}$), hydrogen peroxide (H_2O_2) and hydroxyl radicals ($^{\bullet}OH$) resulting from abiotic stress conditions (Loreto and Velikova, 2001; Vickers et al., 2009). In addition, isoprene can play an intriguing ecological role, contributing to regulate stress-related internal signaling processes (Farmer, 2001; Velikova et al., 2005, 2012), and influencing plant-insect communication (Laothawornkitkul et al., 2008; Loivamaäki et al., 2008; Brilli et al., 2009).

Among the most abundant VOC emitted ubiquitously from vegetation (Loreto and Schnitzler, 2010), methanol is produced during cell expansion, when cell wall pectins are degraded by the action of pectin methylesterase (PME) enzymes (Gaffe et al., 1994). As a water-soluble compound able to dissolve in liquid pools within leaves, methanol emission strongly depends on stomatal conductance (Niinemets et al., 2004). The diurnal rates of cell growth also seem to affect methanol production and emission (Hüve et al., 2007; Oikawa et al., 2011).

Whereas methanol is a quite stable compound in the atmosphere, having a rate constant for gas-phase reaction with $^{\bullet}OH$ of 0.94×10^{12} cm^3 $molecule^{-1}$ s^{-1}, isoprene and monoterpenes are much more reactive, having 100-fold higher $^{\bullet}OH$ reaction time constants (Atkinson and Arey, 2003). Moreover, many isoprenoids have faster reaction time with ozone and thus photochemical reactions often involve both O_3 and isoprenoids. Although ozone is initially destroyed, it is successively regenerated with a final positive balance in favor of O_3. Consequently, when nitric oxides (NO_x), light and high temperature combine, volatile isoprenoids directly contribute to the formation of ground-level ozone (Chameides et al., 1988), particles (Kiendler-Scharr et al., 2009) and secondary organic aerosol (Claeys et al., 2004), thereby affecting air chemistry and air quality at regional and global level. Isoprene oxidation leads to the formation of first-order products, mainly methyl-vinyl ketone (MVK) and methacrolein (MACR) (Pierotti et al., 1990; Pinho et al., 2005). Different field campaigns and laboratory experiments have recently demonstrated that MVK + MACR (referred to here collectively as i_{ox}) can be either taken up (Karl et al., 2010; Misztal et al., 2011) or emitted by the canopy (Langford et al., 2010; Jardine et al., 2012). If an i_{ox} flux exits the canopy, as well as the leaf of a gas-exchange cuvette in which the residency of air is very short, then isoprene undergoes oxidation already within leaves, possibly by reacting with ROS abundantly produced under stressful conditions (Loreto and Velikova, 2001; Jardine et al., 2012; Brilli et al., 2012).

In bio-energy plantations, combined flux measurements of VOC and carbon have to date only been made in an oil palm plantation in south-east Asia (Misztal et al., 2011). Because poplars are increasingly used in bio-energy plantations in the temperate zone (Migliavacca et al., 2009; Cai et al., 2011) and are strong isoprene emitters (Guidolotti et al., 2011), it is important to study their VOC fluxes in relation to site carbon balance and environmental drivers. Here we used a combination of leaf- and ecosystem-scale measurements to collate fluxes of carbon (both as photosynthesis and as VOC) and ozone during two weeks of rapid growth of a poplar plantation in July 2012. The specific objectives of this study were to:

(1) measure ecosystem-level eddy covariance fluxes of a multitude of VOC to investigate how environmental factors influence emissions of multiple VOC and CO_2 uptake in the short-term;
(2) assess how CO_2 uptake through photosynthesis correlates with re-emission of carbon in the form of volatile isoprenoids in juvenile versus adult leaves of five different poplar genotypes;
(3) combine leaf- and ecosystem-level data to quantify the importance of within-plant isoprene oxidation, leading to primary emission of i_{ox}.

2. Materials & methods

2.1. Field study site

The PopFull (http://webh01.ua.ac.be/popfull) experimental bio-energy poplar plantation is located in Lochristi (51°04′44″N, 3°51′02″E) (Belgium) at an elevation of 6 m a.s.l. in a completely flat terrain. Poplars were coppiced in January, 2012 and new shots started to sprout on May, 2012. A more detailed description of the study site as well as footprint analysis is given by Zona et al. (2012, 2013) and Broeckx et al. (2012). In addition, a leaf area index (LAI) = 3.5 ± 1 was directly measured during this study (Sarzi-Falchi et al., personal communication).

2.2. Eddy covariance (EC)

Two eddy covariance systems were installed on the same tower in the north-east corner of the field site:

(1) a greenhouse gasses (GHG)-eddy system was equipped with a sonic anemometer (CSAT-1, Campbell Scientific Inc., Logan, UT, USA) coupled with a closed-path infrared gas analyzer (LI-7000, LI-COR Biosciences Inc., Lincoln, NE, USA) and a chemiluminescence-based fast ozone sensor (model LOZ-3F, Drummond Technology Inc., Ontario, Canada) to measure CO_2, H_2O and O_3 fluxes (Zona et al., 2014). Data recorded from these devices were collected and synchronized with a data-logger (model CR3000 & CR5000, Campbell Scientific Inc.) at 10 Hz sampling frequency (Zona et al., 2012, 2013);
(2) a VOC-eddy system including a sonic anemometer (model USA1, Metek GmbH, Elmshorn, Germany) coupled with a proton transfer reaction "Time-of-Flight" mass spectrometer (PTR–TOF–MS) (Ionicon, Innsbruck, Austria) to measure volume mixing ratios (VMRs) of VOC. The data streams of the anemometer and the PTR–TOF–MS were acquired independently by two different computers and synchronized with a dedicated software (NTP, Network Time Protocol, University of

Delaware, DE, USA) to an independent external clock through the Internet, with an accuracy <20 ms.

The two eddy covariance systems were completely independent, although they were installed very close to each other, with 1 m spatial separation between the inlets of the two sampling lines. Separate Teflon® sampling lines (each one ~15 m long and 8.0 mm ID) for each eddy covariance system were set up.

Here, positive fluxes represent transport from the canopy toward the atmosphere (emission), negative ones the reverse (deposition).

2.3. Eddy covariance fluxes calculation

2.3.1. GHG

The computation of CO_2, ozone, latent heat (LE), sensible heat (H), momentum fluxes was made with the EddyPro software (www.licor.com/eddypro, Fratini et al., 2012). A two-component axis rotation was adopted, while the automatic maximization of cross covariance was used to determine the lag-time for passive scalars, which was about 2 s. A drop-out filter was applied to remove the zeroing periods (10 s h^{-1}) from the 10 Hz dataset of ozone data. Frequency response correction was performed according to the analytical method of Moncrieff et al. (1997) to estimate high frequency attenuation, and according to Moncrieff et al. (2004) for low frequency correction (high pass filtering). A sensor separation correction was applied according to Horst and Lenschow (2009). Data were filtered based on the following criteria: during malfunctioning of the instruments, calibration and maintenance, when electric spikes occurred, and when the wind direction was outside of the footprint of interest (i.e. >250° and <50°).

CO_2 flux was gap-filled and then partitioned into Ecosystem Respiration (RECO) and Gross Primary Production (GPP) using the Marginal Distribution Sampling (MDS) method (Reichstein et al., 2005) implemented in http://www.bgc5jena.mpg.de/~MDIwork/eddyproc/index.php and adopted by FLUXNET for standardized gap-filling and flux-partitioning (Moffat et al., 2007; Papale et al., 2006).

RECO was derived from nighttime net ecosystem exchange (NEE) and then extrapolated to daytime conditions using the regression model of Lloyd and Taylor (1994). Nighttime NEE data were selected using a global radiation threshold of 20 W m^{-2}.

Gross primary production (GPP) was calculated as: $GPP = -|NEE| + |RECO|$

2.3.2. VOC

In order to standardize the computation of VOC fluxes with the eddy-covariance method and thus enable the application of all the required processing steps to a multitude of VOC concentrations (Fig. S3), EddyPro software was modified into a new customized version that we named EddyVoc.

The processing routine programmed in EddyVoc, first masked raw data with a quality flag to exclude individual spikes, values out-of-range (such as negative concentration values) and background calibration periods of the PTR–TOF from further processing. Then, double rotations for tilt correction (Wilczak et al., 2001), linear de-trending (Rannik and Vesala, 1999), time-lag estimation based on the covariance maximization (Aubinet et al., 2000) were performed. Since isoprene exhibited the strongest signal-to-noise ratio in the covariance with vertical velocity during the period of measurements, it was used to compute the 30-min time-lags for all other VOC species, assuming that all VOC were subject to the same physical turbulent transport across the sampling line (Fares et al., 2012). In a final step, corrections for flux loss were applied as sensor separation (Horst and Lenschow, 2009), low frequency correction (Moncrieff et al., 2004). Actual spectral correction factors were calculated according to the model of Ibrom et al. (2007), Eq. (9), parameterized after the refinements of Fratini et al. (2012). Resulting flux correction factor was 1.20 on average (i.e. estimated flux loss of 20%), ranging from about 1 to about 1.6 depending on atmospheric stability and turbulence conditions.

More details on the methodology used for in-situ spectral analysis and flux corrections (Fig. S1) as well as correlation between sensible heat flux measured by the (GHG)-eddy system and VOC-eddy system (Fig. S2), and time-series measurements of volume mixing ratios (VMRs) of VOC (Fig. S3) are given in Supplementary Data.

2.3.3. Quality control

Quality controls on half-hourly fluxes were applied according to Göckede et al. (2004), resulting in an overall quality flag (0 for good data, 1 for acceptable data, 2 for bad data) assigned to each flux value. Friction velocity threshold was estimated at 0.12 m s^{-1} by assessing when the nighttime NEE dependence on u^* reaches saturation. Finally, VOC fluxes random uncertainty was estimated with EddyVoc by using the method of Finkelstein and Sims (2001).

2.4. PTR–TOF–MS set-up and operations

At ecosystem-level, a Proton Transfer Reaction "Time-of-Flight" Mass Spectrometer (PTR–TOF–MS) (Ionicon, Innsbruck, Austria) described by Jordan et al. (2009) and Graus et al. (2010) was used to record high-resolved mass spectra of VOC (up to m/z 315) at high frequency (10 Hz). The whole dataset recorded between 16th and 28th of July was post-processed to screen for the presence of emitted/deposited fluxes of the most common protonated molecules or fragments of VOC, excluding instrumental signals produced by the PTR–TOF–MS itself such as major primary ions (e.g. H_3O^+,·H_2O–H_3O^+) and impurities (e.g. O_2^+, NO^+, NH_4^+). VOC were detected through proton transfer reactions occurring between the H_3O^+ ions produced within the ion source and the air sample inserted into the drift tube which is kept under controlled conditions of: pressure (2.3 mbar), temperature (50 °C) and voltage (600 V) resulting in an ionization energy (E/N) of ≈120 Td. All protonated ions were extracted from the drift tube, pulsed every 30 μs, separated according to their m/z ratio in the time-of-flight region and detected in conjunction with a multi-channel-plate (MCP, Burle Industries Inc., Lancaster, PA, USA).

In our set-up, ambient air was drawn at a constant flow rate of ~30 l min^{-1} through the VOC-eddy system sampling line heated at 40 °C in order to maintain both a higher Reynolds number in the tubing (Re > 6000) and to ensure reduced line pressure that protects against condensation. The last meter of the main pipeline was converted first from 8.00 mm to 1/8′ mm ID and then from 1/8′ to 1/16′ mm ID to match the capillary inlet of the PTR–TOF–MS system.

Raw PTR–TOF–MS data were acquired at 10 Hz sampling rate by the TofDaq software (Tofwerk AG, Switzerland), then merged and averaged to 6 min, and post-processed by routine programs (Müller et al., 2010, 2013). In order to assign an exact mass scale, and later the sum formula to the detected ions, the mass scale accuracy of all the recorded spectra was calibrated by exploiting two well-defined PTR–TOF–MS background ion peaks (m/z = 21.022 and m/z = 39.033 related to H_3O^{18+} and·H_2O-H_3O^{18+}, respectively), and by inserting 1,2,3 trichlorobenzene (m/z = 180.937) to the sample inlet system through a diffusive cell. A more detailed description of the PTR–TOF–MS data analysis is given elsewhere (Müller et al., 2013).

The background signals of the PTR–TOF–MS were quantified for the first 6 min of every hour via an automation system of switching valves that introduced VOC-free air generated by a commercially available gas calibration unit (GCU) (Ionimed, Innsbruck, Austria). The same GCU has been employed to calibrate

the PTR–TOF–MS sensitivity once a week at ambient humidity by adding a multi-component gravimetrically prepared gas standard, containing: methanol (*m/z* 33.033), acetaldehyde (*m/z* 45.033), acetone (*m/z* 59.049), isoprene (*m/z* 69.070), MVK + MACR (*m/z* 71.049), t-2-hexen-1-al (*m/z* 99.081), c-3-hexen-1-ol (*m/z* 101.061) and α-pinene (*m/z* 137.133) at nominal concentration of 1 ppmv each (Apel Riemer, USA). All standards were diluted with VOC-free air in order to achieve various concentration levels of VOC in the low ppb range (1-20 ppb) with the same relative humidity as the sampled ambient air. Sensitivities were extrapolated from linear regressions of the known VOC mixing ratios and the respective signal intensities (thus already including transmission coefficient) after subtracting the average background levels. As proposed by Ruuskanen et al. (2011) we used the average normalized sensitivities for oxygen containing compounds and for pure hydrocarbons to calibrate the VOC that were not present in the gas standard.

2.5. Leaf gas exchange

At leaf level, gas exchange measurements of CO_2 and H_2O were performed daily *in situ* from 23th to 27th of July (2012) between 10:00 and 17:00 by using a portable gas exchange system (LI-COR6400, LI-COR Biosciences Inc., Lincoln, NE, USA) on 5 different *Populus* genotypes (*Grimminge, Koster, Oudenberg, Skado, Wolterson*) placed within the footprint of the eddy covariance tower. In each one of the selected poplar genotypes, 5 ± 1 young leaves (whose expansion was lower than 30% of full leaf expansion, i.e. generally the third leaf expanding from the vegetative apex), and 5 ± 1 mature leaves (fully expanded and generally placed in the middle of the stem, 10–12 leaves from the apex) (Brilli et al., 2009) of 5 ± 1 different trees were chosen. Leaves were clamped in the 6 cm^2 LI-COR cuvette, and photosynthesis (*A*), stomatal conductance (*gs*) and internal CO_2 concentration (*Ci*) were measured using the LI-COR software. All the enclosed leaves were exposed to: saturating photosynthetic photon flux density (PAR) of 1000 $\mu mol\ m^{-2}\ s^{-1}$, CO_2 concentration of 380 ppmv (achieved by fully scrubbing CO_2 from ambient air with soda lime and replacing it with the LI-COR6400 CO_2-injector system), leaf temperature of 25 °C, and relative humidity ranging between 45 and 50%. Respiration rates were measured with the same LI-COR6400 portable gas-exchange system on leaves that had been dark adapted for 30 min following the measurement of net photosynthesis and isoprene emission rate. Gross photosynthesis was defined as: |net photosynthesis| + |respiration|.

2.6. VOC collection and GC–MS analysis

At leaf-level, VOC were detected simultaneously with CO_2 and H_2O gas exchange measurements by concentrating 6 L of the air exiting the cuvette in cartridges filled with 250 mg of Tenax (Markes International Limited, Llantrisant, UK). All VOC were removed from ambient air before flushing the gas exchange cuvette, with a charcoal filter (Supelco, Bellafonte, USA) placed ahead of the LI-COR6400 inlet.

In addition, on 22–28 of July, between 12:00 and 17:00, VOC were also occasionally sampled directly from the EC tower by concentrating 6 L of ambient air in Tenax cartridges.

After collection, all the adsorbed cartridges were thermally desorbed and the released compounds were then detected by gas chromatography-mass spectrometry (GC–MS) (HP5890; Hewlett-Packard, Palo Alto, CA, USA) as shown in detail by Brilli et al. (2009). VOC background was measured every day before starting the measurements by collecting 6 L of air exiting the empty LI-COR6400 cuvette. The GC–MS was calibrated by sampling different concentrations of VOC produced after dilution of the same gas standard (Apel Riemer, USA) by the GCU device, as described above. Both leaf- and ecosystem-level GC–MS analysis unambiguously confirmed that the signal at *m/z* = 69.070 detected by PTR–TOF–MS and assigned here to isoprene did not have any interference from the fragment of 2-methyl-1-butanol, which have the same exact mass weight.

2.7. Ancillary data

Supporting meteorological measurements were recorded continuously and data were stored in several data loggers (model CR3000, CR5000 and CR1000; Campbell Scientific, Logan, Utah, USA); in particular: Incoming PAR was measured above the canopy using a quantum sensors (Li-190; LI-COR, Lincoln, NE, USA); air temperature (T_{air}) and water pressure deficit (VPD) were recorded at 6-m height on the eddy covariance tower; volumetric soil water content (SWC) was assessed at 0.1-m depth in the proximity of the eddy covariance installation, by time domain reflectrometry (TDR model CS616; Campbell Scientific, Logan UT, USA); precipitation was recorded by using a tipping bucket rain gauge (model 3665R; Spectrum Technologies Inc., Plainfield, IL, USA); NO_x concentrations were measured by using a Chemoluminescent $NO/NO_2/NO_x$ analyser, model 42i (Thermo Fisher Scientific, Aalst, Belgium).

Ecosystem flux parameters were best-fitted with light, temperature and VPD by using SigmaPlot version 11.0 (Systat Software Inc., San Jose, CA, USA).

3. Results

3.1. Climate and meteorological data

Two very different meteorological conditions characterized the measurements period (Fig. 1). During the initial days (16–21 of July) measurements were carried out under overcast sky and a cold temperature regime (~15 °C), with few small rainfall events (Fig. 1b). During this period, the maximum incoming PAR flux remained less than 700 $\mu mol\ m^{-2}\ s^{-1}$ (Fig. 1a).

A change in wind speed, direction, and turbulence occurred during the night of 20th of July (Fig. 1c and d), without any immediate change in temperature. However, during the following night (22th of July), the sky cleared up as confirmed by a drop in temperature that reached the minimum value of ~9 °C at 06:00 (Fig. 1a). All the following days of measurements (22–28 July) were characterized by good weather conditions, high incoming PAR fluxes (reaching maximum intensity of ~1500 $\mu mol\ m^{-2}\ s^{-1}$ at noon), air temperatures rising to 28 °C (Fig. 1a) and absence of rainfall (Fig. 1b). Higher air temperatures recorded during the second part of the measurements period also triggered an increased evaporative demand (i.e. increased VPD) of the atmosphere (Fig. 1e). In this second part of the experiment, a drop in PAR was registered during every afternoon (at around 18:00) as a consequence of low altitude cloud formation from water vapor condensation occurring during the hottest hours of the day (Fig. 1a). Despite this change in weather conditions, soil water content (SWC) level remained high and fairly constant throughout the entire study period (Fig. 1b), thus excluding any drought impact.

Whilst during the initial cold period of measurements (16–21 July) compounds such as ozone (O_3), nitric oxide (NO) and nitrogen dioxide (NO_2) (together referred to as NO_x) were almost totally absent at the site (Fig. 1f and g), NO_x concentration increased starting from 20th of July morning.

3.2. Fluxes at ecosystem-level

Patterns of gross primary production (GPP) displayed no significant changes during the whole period of investigation, regardless of

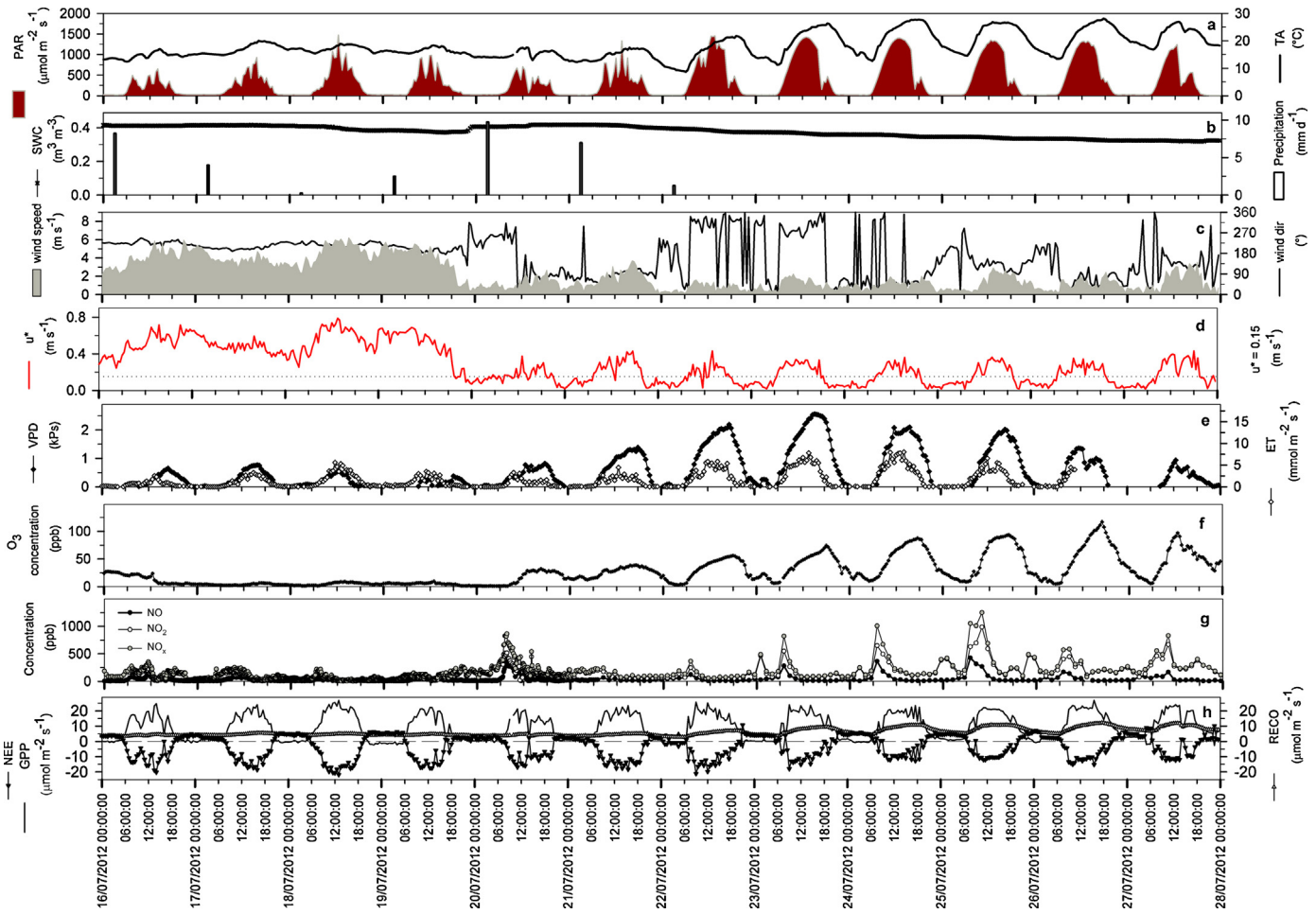

Fig. 1. Meteorological and physiological characterisation of the measured period at the field site from 16 to 28 July (2012), showing half-hour averages of: (a) incident photosynthetically active radiation (PAR) and air temperature (TA), (b) volumetric soil water content (SWC; at 0.1 m depth) and daily totals of precipitation, (c) wind speed and wind direction, (d) friction velocity (u^*) and friction velocity threshold $u^* < 0.15\ m\ s^{-1}$, (e) vapour pressure deficit (VPD) and evapotraspiration (ET), (f) O_3, (g) NO, NO_2, NO_x concentrations in ambient air, (h) net ecosystem CO_2 exchange (NEE), night time ecosystem respiration (RECO) and gross primary production (GPP).

the increases in PAR and temperature that occurred during the second measuring period (Fig. 1h). However, net ecosystem exchange (NEE) was considerably reduced during the latest part of the campaign by an increase in ecosystem respiration (RECO) resulting in a relatively constant values of GPP (Fig. 1h; Table 1).

Fluxes of the protonated ions $m/z = 33.033$ and m/z 69.070, corresponding to methanol and isoprene, respectively, were clearly detected from 22th of July onwards, following the increase of PAR and temperature (Fig. 1a; Fig. 2; Fig. 3; Table 1). To a lesser extent, fluxes of other oxygenated-protonated ions were also detected as: $m/z = 31.018$ (formaldehyde), $m/z = 45.034$ (acetaldehyde), $m/z = 59.049$ (acetone), $m/z = 61.028$ (acetic acid), $m/z = 71.049$ (i_{ox}), $m/z = 73.068$ (methyl ethyl ketone, MEK). Flux measurements indicated that isoprene was always emitted from the canopy (Fig. 2). Other oxygenated-VOC were either released into the atmosphere or deposited to the vegetation, (Figs. 2 and 3), although methanol was also mainly emitted except for some small deposition events (Fig. 3).

Isoprene was the most abundant VOC emitted from the poplar plantation (Fig. 2; Table 1). Its exchange with the atmosphere displayed a diurnal trend that was more pronounced in the warmer than in the cold period (Fig. 3; Table 1). Isoprene always started to be emitted at dawn (~6:00), and emissions peaked twice during the day: first at noon in correspondence with the maximum of PAR, and then between 15:00 and 16:00 when the temperature rose to its maximum (and light was less intense but more scattered due to the presence of low clouds). Both peak emissions of isoprene reached a similar rate of 6.62 ± 1.20 and $6.78 \pm 1.47\ nmol\ m^{-2}\ s^{-1}$ (Fig. 3; Table 1). After the second peak, isoprene emission started to decline, approaching zero in the evening, at ~20:00 (Fig. 3; Table 1). The isoprene flux increased exponentially with temperature ($f(x) = q\ e^{kx}$, Table 3) and logarithmically with PAR (Fig. 4a, b, respectively). In contrast to isoprene emissions, GPP saturated at ~400–500 $\mu mol\ m^{-2}\ s^{-1}$ of PAR (Fig. 4d), and also showed a more complex logarithmic relationship rather than an exponential relationship with temperature than isoprene (Fig. 4c).

An exponential relationship was found that linked ecosystem GPP to isoprene emission. This relationship was not affected by the switch between the first cold and the second warmer period (Fig. 5b and c).

Along with isoprene, half-hourly averages methanol fluxes also exhibited a very clear diurnal cycle during the warm measurement period (Fig. 3). Emissions started at 6:00 and peaked twice: at noon and at ~16:00, before decreasing slowly until 20:00 thus mirroring the daytime course of PAR and air temperature (Fig. 3). In contrast to isoprene fluxes, the first methanol peak emission reached a higher rate ($5.82 \pm 0.29\ nmol\ m^{-2}\ s^{-1}$) with respect to the second peak ($4.46 \pm 0.49\ nmol\ m^{-2}\ s^{-1}$; Fig. 3, Table 1). As for isoprene, between the two peaks of methanol, a singular event of reduced emission occurred at ~14:00 when PAR started to decline. In order to explore the environmental control on the methanol flux, we tested the relationships with the main meteorological variables:

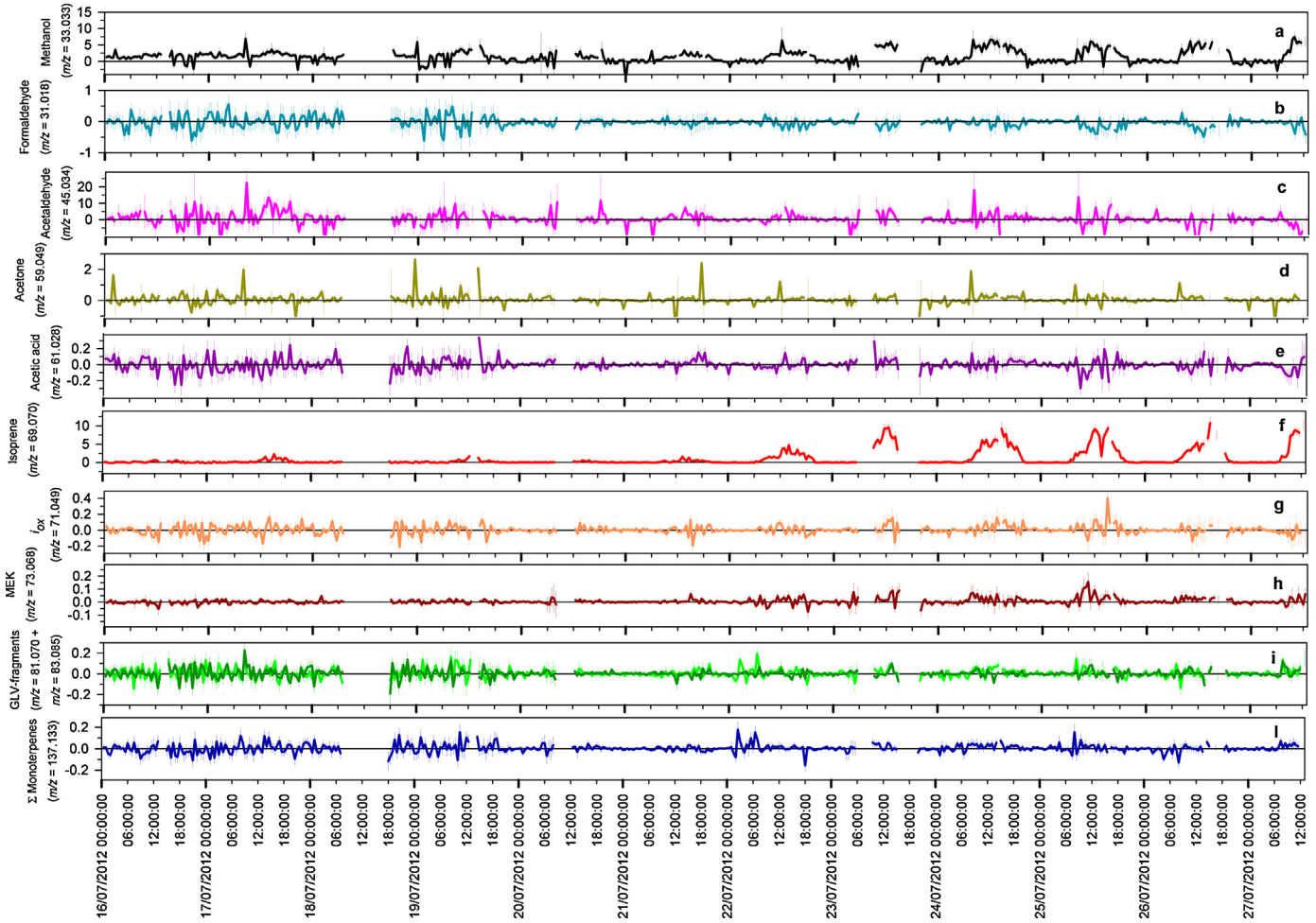

Fig. 2. Time series of half-hourly VOC fluxes measured by PTR–TOF–MS at the field site during the whole period (16–28 July, 2012). Vertical bars indicate random uncertainty associated to each measured half-hour average flux.

VPD, (Fig. 6a), PAR (Fig. 6b) and temperature (Fig. 6c). A simple linear regression described best the correlation between methanol flux and VPD ($R^2 = 0.29$, Table 3; Fig. 6a), whereas a logarithmic response was found between methanol flux and PAR ($R^2 = 0.40$, Table 3; Fig. 4b), as well as between methanol flux and temperature ($R^2 = 0.25$, Table 3; Fig. 6c).

Formaldehyde was only deposited to the vegetation, whereas MEK was emitted during the warmest days (Fig. 3; Table 1). Moreover, bi-directional exchange of other oxygenated VOC such as acetone, acetaldehyde and acetic acid were measured throughout the day during the whole period of measurements (Figs. 2 and 3; Table 1). In particular, a combined burst of acetaldehyde and acetone emission always occurred in the morning, at 8:00–8:30 (Fig. 3). Similarly, measured fluxes of i_{ox} seemed to be bi-directional, alternating short period of deposition and of emission (Fig. 2). Nonetheless, emissions of i_{ox} peaked together with those of isoprene during both the cold and the warm measurement period (Fig. 3) and also their temperature dependencies were comparable (Fig. 4a and 7b). Concentrations of i_{ox} collected at the tower during the warm measurement period ($25 \pm 1\,^{\circ}C$) linearly correlated with isoprene concentrations ($R^2 = 0.49$, Table 3), suggesting i_{ox} to account for ~32% of isoprene (Fig. 7a, Table 3). In addition, fluxes of both i_{ox} and isoprene measured under different temperatures ranging from ~8 to ~28 °C fitted the function: $i_{ox} = \text{isoprene}\ T^{power}$ resulting in an exponential (power) value of 3.8 ± 0.4 (Fig. 7b, Table 3).

A protonated ion-flux was detected at $m/z = 81.070$, suggesting a flux of either a monoterpene or a main green leaves volatiles (GLVs) fragment. Unfortunately, both fluxes of molecular monoterpene ions ($m/z = 137.133$) and of another main GLVs fragment ($m/z = 83.085$) showed values very close to the associated random uncertainties, making difficult any discussion about monoterpene fluxes at plantation-level (Fig. 2; Table 1).

During the warming days the ambient concentration of ozone measured at the site increased 5-fold, and NO_x increased 10-fold with respect to the first cold period, from a daily average concentration of 8.12 ± 1.41 to 78.89 ± 3.62 ppbv for ozone (Fig. 1f) and from 25.15 ± 1.41 to 268.16 ± 22.11 ppbv for NO_x (Fig. 1g). As a consequence, the poplar plantation started uptaking tropospheric ozone during the second part of our measurement campaign (Fig. 3; Table 1). Ozone deposition started in the morning at 6:00 (along with methanol and isoprene emission) (Fig. 3), and peaked between noon and 16.00, when the deposition rate was constant at 17.02 ± 0.76 nmol m^{-2} s^{-1} (Fig. 3). Minimal ozone deposition was observed starting at 20:00 and throughout the night.

3.3. Fluxes at leaf-level

On average, juvenile leaves showed lower photosynthesis (3.22 ± 0.53 μmol m^{-2} s^{-1}) and higher dark respiration rates (7.78 ± 0.42 μmol m^{-2} s^{-1}) than adult leaves (photosynthesis ~15.76 ± 0.42 μmol m^{-2} s^{-1} and respiration

Table 1
Summary statistics for eddy covariance fluxes of VOC, O_3 GPP, NEE above the poplar plantation and parameters of light and temperature measured during the two consecutive periods (16–21 and 22–28 July, 2012) of intensive campaign. In parenthesis are given statistics values for fluxes that have successfully passed all the quality criteria mentioned in Section 2.3.3.

	Light (μmol m^{-2} s^{-1})	Temperature (°C)	NEE (μmol m^{-2} s^{-1})	O_3 (nmol m^{-2} s^{-1})	Methanol (nmol m^{-2} s^{-1}) m/z = 33.033 CH_4O-H^+	Formaldehyde (nmol m^{-2} s^{-1}) m/z = 31.018, CH_2O-H^+	Acetaldehyde (nmol m^{-2} s^{-1}) m/z = 45.034, C_2H_4O-H^+	Acetone (nmol m^{-2} s^{-1}) m/z = 59.049, C_2H_4O-H^+	Acetic acid (nmol m^{-2} s^{-1}) m/z = 61.029, C_3H_6O-H^+	Isoprene (nmol m^{-2} s^{-1}) m/z = 69.070, C_5H_8-H^+	i_{ox} (nmol m^{-2} s^{-1}) m/z = 71.049, C_4H_6O-H^+	MEK (nmol m^{-2} s^{-1}) m/z = 73.068, C_4H_8O-H^+	GLV & monoterpenes fragment (nmol m^{-2} s^{-1}) m/z = 81.070, C_6H_8-H^+	m/z 83.085 (GLV fragment) (nmol m^{-2} s^{-1}) m/z = 83.085, C_5H_{10}-H^+	Σ Monoterpenes (nmol m^{-2} s^{-1}) m/z = 137.133, $C_{10}H_{16}$-H^+
16–21/07/12															
Mean	170 (280)	15.49 (16.2)	−4.46 (−5.45)	−1.09 (−1.12)	1.20 (1.34)	−9.99 E10^{-3} (−3.47 E10^{-3})	0.84 (0.72)	0.08 (0.09)	E10^{-2} (−6.74 E10^{-3})	0.18 (0.31)	E10^{-3} (1.82E10^{-3})	E10^{-3} (−6.74 E10^{-3})	−3.28 E10^{-3} (1.17)	−3.28 E10^{-3} (−0.01)	−2.11 E10^{-3} (−9.74 E10^{-5})
Median	244 (206)	15.71 (16.1)	−3.70 (−6.36)	−1.15 (−0.28)	1.39 (1.56)	−1.61 E10^{-2} (−3.59 E10^{-3})	0.34 (1.06)	0.03 (0.04)	7.84 E10^{-3} (−1.44 E10^{-3})	0.06 (0.16)	2.07 E10^{-3} (0.01)	1.25 E10^{-3} (−1.63 E10^{-3})	−2.38 E10^{-3} (1.61)	−2.38 E10^{-3} (−0.01)	−4.29 E10^{-3} (−2.11 E10^{-3})
95th percentile	618 (916)	17.33 (18.9)	3.75 (5.45)	0.24 (1.36)	3.26 (3.13)	0.33 (0.36)	8.09 (9.79)	0.48 (0.62)	0.33 (0.17)	0.86 (1.18)	0.10 (0.12)	0.02 (0.02)	0.10 (3.43)	0.09 (0.11)	0.08 (0.08)
5th percentile	23 (21)	14.26 (13.4)	−15.01 (−17.61)	−2.54 (−6.51)	−1.52 (−1.75)	−0.32 (−0.41)	−5.16 (−5.70)	−0.29 (−0.35)	−0.23 (−0.16)	−0.11 (−0.06)	−0.09 (−0.15)	−0.02 (−0.02)	−0.06 (−2.31)	−0.07 (−0.14)	−0.07 (−0.08)
SE	34 (19)	0.16 (0.1)	1.05 (0.56)	0.14 (0.19)	0.09 (0.15)	0.01 (0.02)	0.26 (0.67)	0.02 (0.05)	0.01 (0.01)	0.02 (0.03)	3.00 E10^{-3} (9.07 E10^{-3})	7.52 E10^{-4} (1.00 E10^{-3})	2.96 E10^{-3} (0.25)	3.10 E10^{-3} (0.01)	3.10 E10^{-3} (4.54 E10^{-3})
N	289 (225)	289 (225)	289 (225)	289 (225)	261 (126)	255 (121)	254 (123)	251 (130)	255 (121)	253 (47)	253 (72)	255 (93)	253 (72)	248 (41)	240 (121)
22–28/07/12															
Mean	451 (783)	20.12 (25.01)	−2.96 (−6.71)	−4.08 (−6.71)	1.56 (4.03)	−0.06 (−0.08)	0.06 (0.57)	0.39 (0.04)	E10^{-3} (−4.60 E10^{-3})	1.51 (4.22)	0.01 (0.02)	0.01 (0.01)	0.01 (3.77)	E10^{-3} (0.02)	0.01 (0.01)
Median	252 (783)	20.83 (25.64)	−2.58 (−6.71)	−2.01 (−6.71)	0.61 (4.48)	−2.09 E10^{-3} (−8.72 E10^{-2})	0.06 (3.05 E10^{-5})	0.03 (0.09)	3.29 E10^{-3} (−7.67 E10^{-3})	0.04 (3.50)	−1.18 E10^{-4} (0.02)	3.23 E10^{-3} (0.02)	3.99 E10^{-3} (3.80)	1.87 E10^{-3} (0.02)	2.75 E10^{-3} (0.02)
95th percentile	1254 (1332)	25.41 (27.58)	4.55 (1.15)	0.40 (2.52)	5.81 (6.28)	0.11 (0.08)	5.22 (5.57)	2.65 (0.41)	0.22 (0.09)	7.39 (9.29)	0.09 (0.13)	0.06 (0.08)	0.07 (6.19)	0.05 (0.06)	0.06 (0.05)
5th percentile	19 (71)	13.36 (21.03)	−12.39 (−12.73)	−12.55 (−17.02)	−1.16 (1.82)	−0.31 (−0.29)	−4.86 (−2.38)	−0.17 (−0.08)	−0.16 (−0.11)	−0.04 (1.18)	−0.07 (−0.11)	−0.03 (−0.05)	−0.04 (1.67)	−0.04 (−0.02)	−0.04 (−0.01)
SE	69 (57)	0.62 (0.29)	0.92 (0.55)	0.62 (0.76)	0.14 (0.54)	7.52 E10^{-3} (0.02)	0.21 (0.54)	0.09 (0.09)	7.15 E10^{-3} (0.01)	0.16 (0.40)	3.23 E10^{-3} (0.01)	1.95 E10^{-3} (6.12 E10^{-3})	2.50 E10^{-3} (0.37)	1.91 E10^{-3} (0.01)	2.53 E10^{-3} (0.01)
N	289 (225)	289 (225)	289 (225)	289 (225)	261 (38)	244 (37)	246 (42)	255 (46)	244 (37)	253 (46)	247 (48)	244 (37)	243 (21)	215 (16)	200 (35)

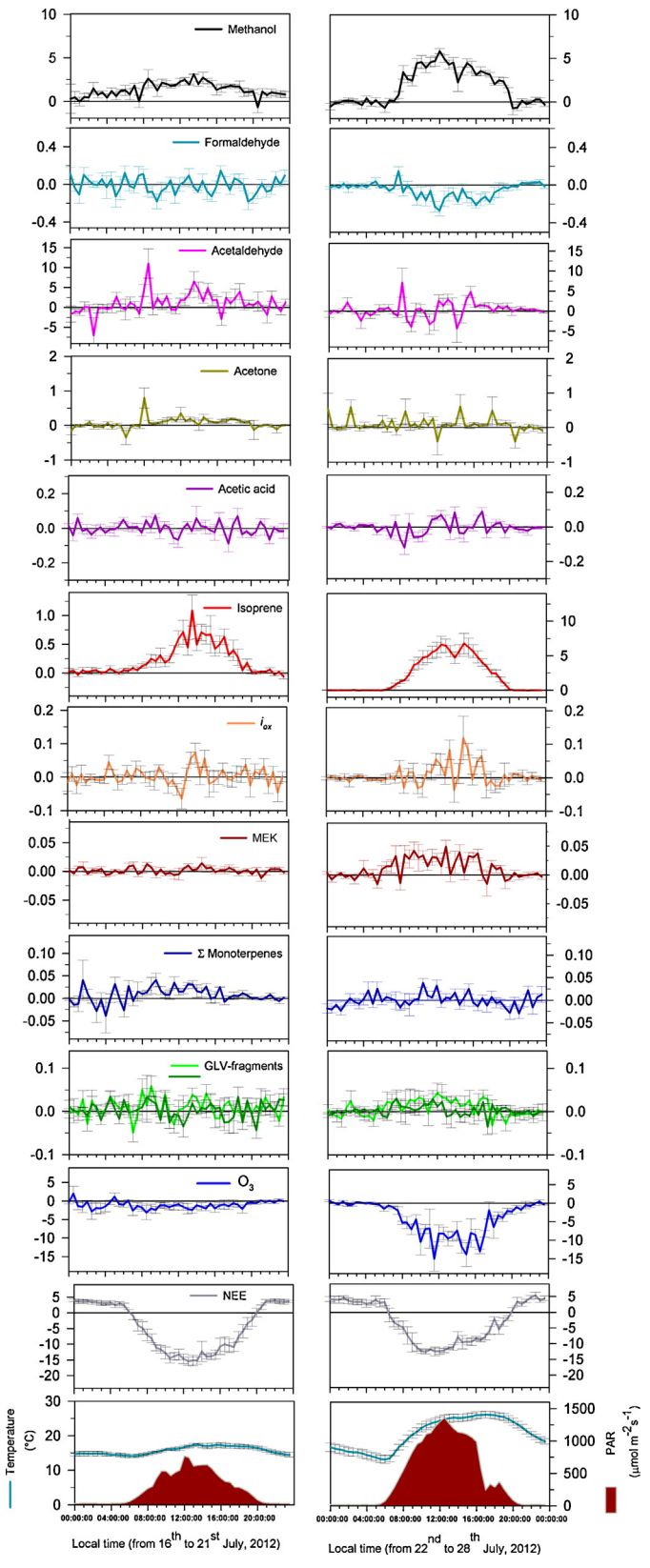

Fig. 3. Diurnal cycles of half-hourly average VOC fluxes measured by PTR–TOF–MS at the filed site during the *consecutive* periods 16–21 and 22–28 of July (2012). Only isoprene fluxes have been plotted in (left- and right-) panels showing different *Y*-scales. Error bars indicate day-to-day variability (standard deviation).

$\sim 3.07 \pm 0.20\ \mu mol\ m^{-2}\ s^{-1}$) (Table 2). Both adult and juvenile leaves exhibited very similar rates of photosynthesis and respiration rates across the five investigated poplar genotypes (Table 2). Above-average dark respiration was found only in juvenile leaves of Koster ($9.25 \pm 0.90\ \mu mol\ m^{-2}\ s^{-1}$) and in adult leaves of Oudenberg ($3.00 \pm 0.23\ \mu mol\ m^{-2}\ s^{-1}$) (Table 2). The highest stomatal conductance was found in adult leaves of Wolterson ($0.537\ mol\ m^{-2}\ s^{-1}$).

Isoprene emission did not statistically differ among the adult leaves of the five investigated poplar genotypes, all ranging around $16\ nmol\ m^{-2}\ s^{-1}$ (Table 2). Isoprene emission was very low in juvenile leaves of all genotypes, with the exception of Skado that showed a slightly higher emission of $\sim 1.25\ nmol\ m^{-2}\ s^{-1}$ (Table 2). A good exponential relationship ($R^2 = 0.68$, Fig. 5a, Table 3) was found between GPP and isoprene emission in both juvenile and adult leaves. These leaf measurements, carried out by using a VOC-free air and at a constant temperature of $25 \pm 1\ ^\circ C$, showed a much lower i_{ox} synthesis, and a lower linear correlation with isoprene emission ($f = ax + b$) with respect to that found at canopy level ($a = 0.073$ and 0.32, respectively, Fig. 7a; Table 3), suggesting that only ~7.3% of isoprene was oxidized in the leaves inserted in the cuvettes.

Monoterpenes were emitted by young leaves of all investigated genotypes (Table 2), but Wolterson and Oudenberg had statistically higher emissions (0.13 ± 0.08 and $0.33 \pm 0.10\ nmol\ m^{-2}\ s^{-1}$, respectively) than the other genotypes (Table 1). Adult leaves emitted no monoterpenes, except for those of the Oudenberg genotype, which emitted trace amounts ($0.05 \pm 0.04\ nmol\ m^{-2}\ s^{-1}$). In all cases, only α-, β-pinene and (*E*)-β-ocimene were detected.

4. Discussion

The present study provides original information on ecosystem- and leaf-level exchange of VOC between a poplar-based SRC plantation and the atmosphere in relation with photosynthesis during the peak of the growing season under changing weather conditions.

4.1. Fluxes at ecosystem-level

4.1.1. Isoprene

We confirm that the most abundant VOC emitted from the poplar plantation was isoprene, consistent with pioneer field studies (Fuentes et al., 1999). Isoprene emission fluxes always displayed a clear diurnal cycle, with two peaks (at and just after noontime), albeit only during the warm days (Fig. 3). This diel pattern was similar to that observed in an aspen forest (Fuentes et al., 1999), but contrasts with the diel pattern observed in an isoprene-emitting oil palm plantation (Misztal et al., 2011). In our study, the two peaks in the isoprene emission coincided with maximum PAR and with the highest temperature, which occurred at different times of the day (at ~12:00 and at ~15:00, respectively). It is unlikely that daytime isoprene emission has been limited by the amount of carbon assimilated through photosynthesis during the period of measurements. Indeed GPP was very similar during the cold and the warm period, whereas isoprene emissions differed substantially between these two periods (Fig. 1h and Fig. 3). Moreover, the absence of GLVs fluxes and the good levels of SWC recorded during the whole period of measurements confirmed that the poplar plantation was not affected by the onset of either biotic (i.e herbivores) or abiotic (i.e. drought) stress conditions that could have altered the rates of isoprene emission (Brilli et al., 2007, 2009).

The occurrence of a dramatic shift in the meteorological conditions (from cloudy sky and low temperatures in the first half of the measurement period to high incoming PAR coupled with rising temperatures in the second half) enabled us to explore the response

Table 2
Leaf-level net photosynthesis (*A*), respiration (R_d), stomatal conductance (g_s), intercellular CO_2 concentration (*Ci*), isoprene and monoterpenes emission in adult and juvenile leaves of plants belonging to 5 different genotypes and their total average. Values represent means of four plants belonging to the same poplar genotype ±1 standard deviation of the mean; different uppercase letters indicate significant differences at $p < 0.05$ among different poplar genotypes.

	Grimminge		Koster		Oudenberg		Skado		Wolterson		Average	
	Adult	Juvenile	Adult	Juvenile	Adult	Juvenile	Adult	Juvenile	Adult	Juvenile	Adult	Juvenile
A ($\mu mol\ m^{-2}\ s^{-1}$)	-15.42 ± -0.59^a	-2.94 ± -1.29^a	-16.78 ± -0.40^a	-2.82 ± -1.13^a	-16.47 ± -1.17^a	-0.86 ± -0.64^a	-14.17 ± -1.41^a	-4.57 ± -0.92^a	-15.97 ± -0.53^a	-4.91 ± -1.14^a	-15.76 ± -0.42^a	-3.22 ± -0.53^a
R_d ($\mu mol\ m^{-2}\ s^{-1}$)	3.37 ± 0.62^a	7.51 ± 0.69^{ab}	2.60 ± 0.33^a	9.25 ± 0.90^b	3.00 ± 0.23^b	8.64 ± 0.56^{ab}	3.85 ± 0.34^a	7.82 ± 0.99^{ab}	2.53 ± 0.40^a	5.69 ± 0.46^a	3.07 ± 0.20^a	7.78 ± 0.41^a
g_s ($mol\ m^{-2}\ s^{-1}$)	0.411 ± 0.049^{ab}	0.127 ± 0.013^a	0.431 ± 0.013^a	0.233	0.426 ± 0.058^{ab}	0.092 ± 0.009^a	0.197 ± 0.025^a	0.147 ± 0.017^a	0.537 ± 0.008^b	0.147 ± 0.024^a	0.400 ± 0.029^a	0.149 ± 0.013^a
				0.023[a]								
Ci (ppm)	273 ± 7^b	335 ± 13^{ab}	268 ± 6^b	339 ± 14^{ab}	283 ± 6^b	349 ± 15^b	225 ± 9^a	320 ± 6^{ab}	255 ± 1^{ab}	288 ± 7^a	261 ± 6^a	327 ± 7^a
Isoprene emission ($nmol\ m^{-2}\ s^{-1}$)	13.08 ± 1.42^a	0.06 ± 0.06^a	10.50 ± 0.78^a	0.11 ± 0.06^a	11.02 ± 1.23^a	0.32 ± 0.10^a	13.15 ± 4.78^a	1.25 ± 0.27^b	7.07 ± 2.14^a	0.27 ± 0.27^a	10.96 ± 1.12^a	0.40 ± 0.12^a
Monoterpenes emission($nmol\ m^{-2}\ s^{-1}$)	n.d.	$0.02^{1} \pm 0.02^{ab}$	n.d.	$0.01^{2} \pm 0.01^a$	$0.05^{3} \pm 0.04^a$	$0.33^{4} \pm 0.10^b$	n.d.	$0.03^{5} \pm 0.02^{ab}$	n.d.	$0.23^{6} \pm 0.05^{ab}$	n.d.	0.10 ± 0.03^a

[1] β-pinene.
[2] (*E*)-β-Ocimene.
[3] (*E*)-β-Ocimene.
[4] α,β-pinene + (*E*)-β-ocimene.
[5] α-Pinene.
[6] α,β-Pinene + (*E*)-β-ocimene.

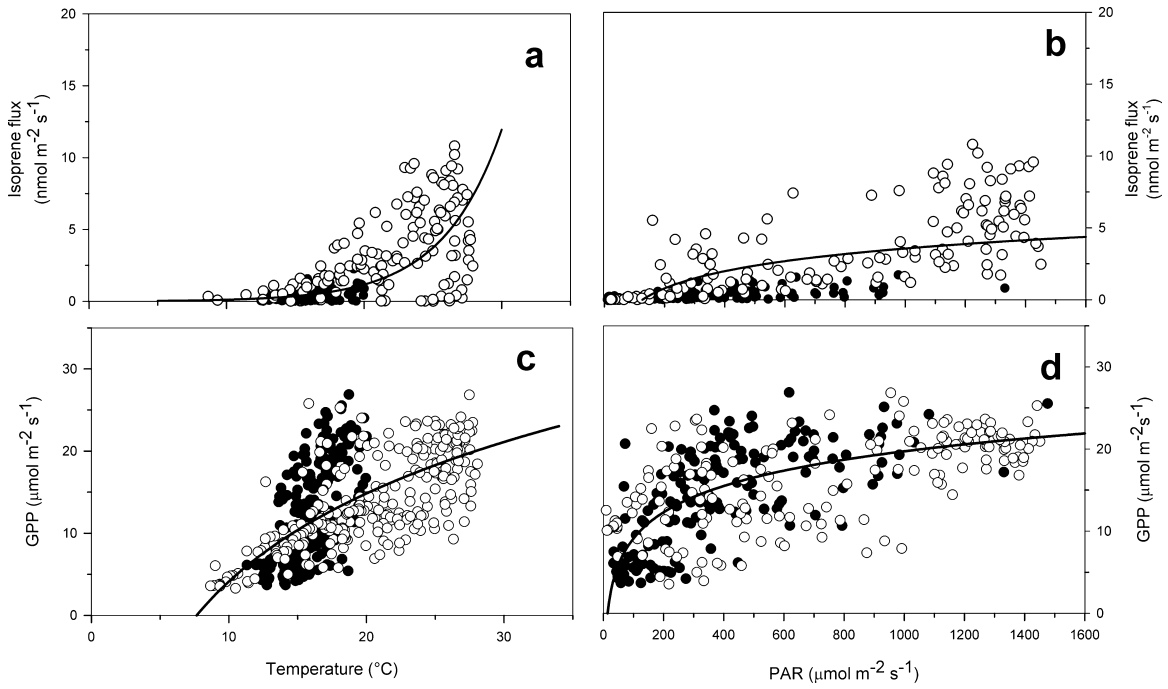

Fig. 4. Isoprene flux as a function of temperature (a), and light (b), and gross primary production (GPP) as a function of temperature (c), and light (d), on a half-hourly time scale. Closed and open symbols are fluxes measured from 16–21 and from 22–28, July (2012), respectively. In (b) and (d) only data from 6:00 to 20:00 have been considered.

of the isoprene flux to a wide fluctuation of both temperature and PAR. Our results are consistent with both field studies (Fuentes et al., 1999) and laboratory investigations (Monson et al., 1992) demonstrating that when isoprene emission is not limited by photosynthesis, it is strictly controlled in the short-term at metabolic level by temperature regimes and PAR. In particular, while temperature affects the optimum for isoprene synthase (IspS) enzymatic activity, PAR provides the amount of reducing power (NADPH) as well as ATP required for isoprene biosynthesis (Sharkey et al., 2008). However, the magnitude of the isoprene flux at plantation level in our study was lower than that measured by Fuentes et al. (1999). One reason could be that the whole plantation was in a juvenile status when our measurements were carried out, as new poplar shoots started to regrow only at the beginning of May after coppicing in January of the same year (2012). The very high respiration rates we detected in juveniles poplar leaves together with high methanol emission we found at ecosystem-level and the increasing values of LAI measured during our investigation (Sarzi-Falchi et al., personal communication) directly support this hypothesis. As a result, in our study the rate of isoprene emission might have been limited by the seasonal development of IspS expression and activity (besides IspS precursors and amount) (Mayrhofer et al., 2005). This was possibly further mediated by growth under conditions of low temperature which could have delayed the plantation capacity to achieve maximum isoprene emission rates (Wiberley et al., 2005).

Interestingly, despite a lower emission rate, isoprene fluxes measured in our study showed a higher temperature dependence that that reported by Fuentes et al. (1999). In fact the temperature sensitivity of isoprene emitted from the poplar plantation resulted in a Q_{10} value of ~10 ($Q_{10} = e^{10 \times 0.23}$, Fig. 4a; Table 3), whereas a Q_{10} of ~2.7 was assessed in a boreal aspen forest ($Q_{10} = e^{10*0.1}$) (Fuentes et al., 1999). However, recent experiments have demonstrated that temperature dependency of isoprene emission is temporarily suppressed during recovery after drought events (Fortunati et al., 2008). Therefore the higher temperature sensitivity of isoprene found in our study with respect to that of Fuentes et al. (1999) was likely due to the short-time resolution of our investigation which have limited the collection of isoprene fluxes only to a period where stressful conditions did not occur. Differently, Fuentes et al. (1999) extrapolated the effect of temperature from seasonal variations of isoprene emission, where fluxes of isoprene measured also during the recovery periods following stress events may have been considered (1999). In addition, the large number of young leaves present in the canopy that we have sampled may have further changed the temperature sensitivity of isoprene with respect to the fully-developed canopy measured by Fuentes et al. (1999). Whether isoprene emission has a higher sensitivity to temperature in juvenile than in adult leaves still needs to be elucidated. Moreover, a potential interference due to a different correlation between the measured air temperature and the actual leaf temperature could have affected the estimation of Q_{10}.

4.1.2. Methanol

Methanol was the second most abundant VOC emitted from the poplar plantation. Consistent with recent studies (Hörtnagl et al., 2011; Laffineur et al., 2011) our results showed a diurnal evolution of methanol efflux from the ecosystem, with emissions occurring between 6:00 and 20:00. As with the isoprene emissions, we observed a double peak in the diel pattern that matched the diel increase of both PAR and temperature (Folkers et al., 2008), and was therefore more clearly visible during the warm days. Moreover, similarly to previous investigations across different ecosystems (Hörtnagl et al., 2011; Laffineur et al., 2011), the variation of environmental parameters recorded in our study could only partially explain the variation in the methanol flux (relation with temperature: $R^2 = 0.25$, with VPD: $R^2 = 0.29$, and with PAR: $R^2 = 0.40$, Fig. 6; Table 3). Temperature determines the rate of methanol production by influencing cell division and expansion through the availability of biosynthetic intermediates and pectin methylesterases (PMEs) enzyme activity (Nemecek-Marshall et al., 1995), and affecting methanol partitioning among the aqueous and gaseous pools in the leaves (Niinemets and Reichstein, 2003). However, these physiological and physicochemical processes influence simultaneously methanol production and emission in a complex regulatory mechanism. Therefore, quantification of PMEs activity in relationship with methanol fluxes (Frenkel et al., 1998; Oikawa

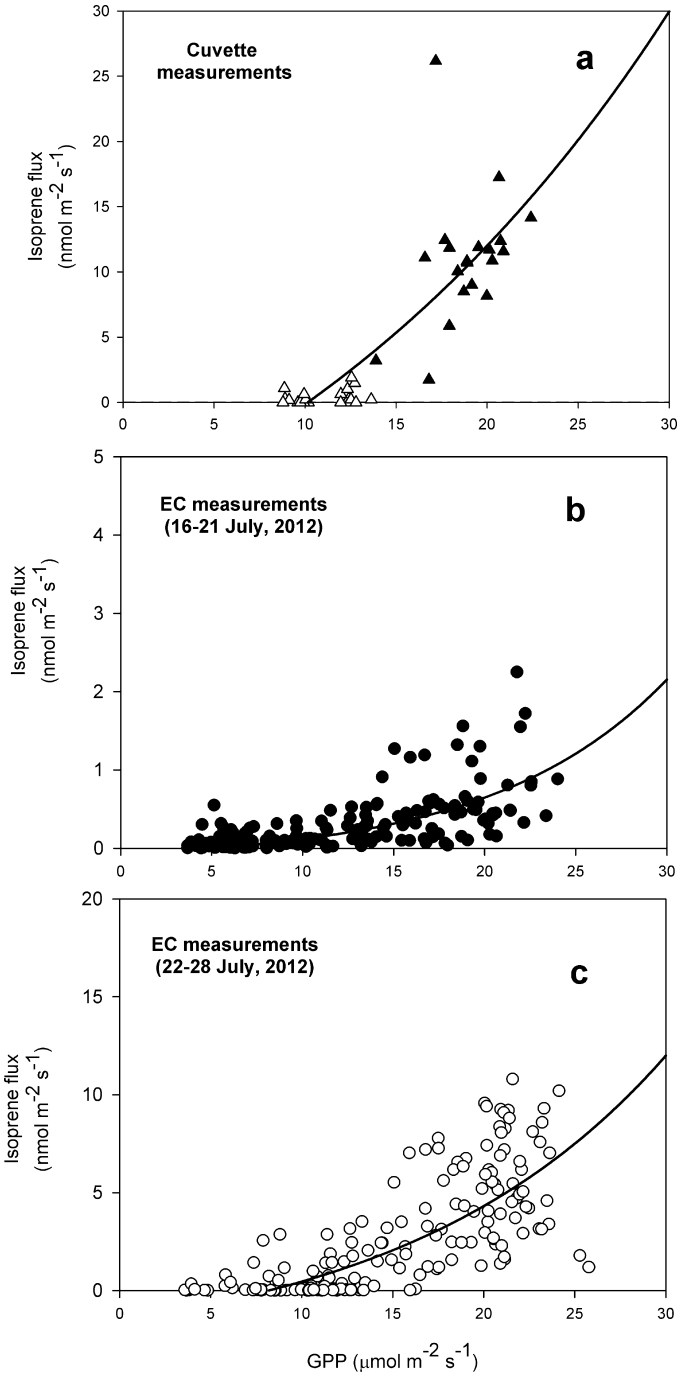

Fig. 5. Leaf-level (a) gross photosynthesis as a function of isoprene emission in juvenile- (open triangle) and adult- (closed triangles) growth stage; (b) ecosystem-level gross primary production (GPP) as a function of isoprene measured from 16 to 21 (open circles) and (c) measured from 22 to 28 (closed circles), July (2012).

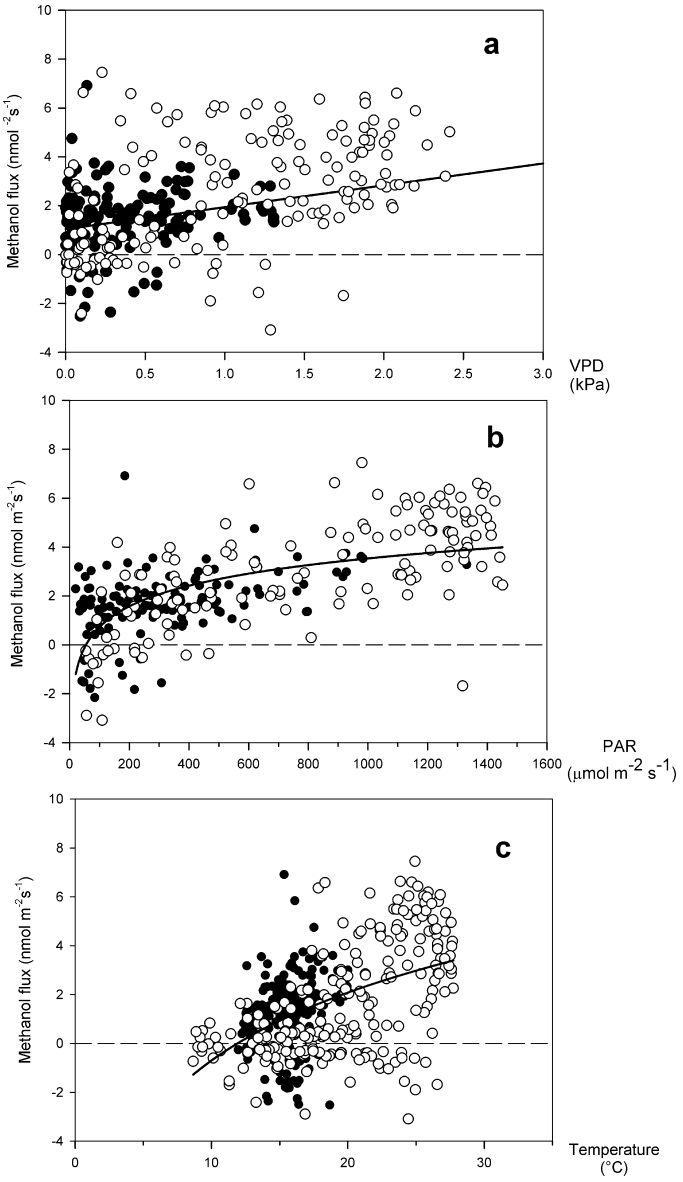

Fig. 6. Methanol flux (a) as a function of VPD, (b) as a function of light and (c) as a function of temperature on a half-hourly time scale. Open symbols are fluxes measured from 16 to 21 and closed symbols are fluxes measured from 22–28, July (2012).

et al., 2011) would be an important parameter to be considered in the future research to precisely dissect the abiotic and biotic control on methanol emission. In particular, during periods of intensive leaf expansion, endogenous biotic drivers (i.e. cell division and cell wall hardening) may easily offset the pure physical analogy recently developed to model methanol fluxes on the basis of adsorption/desorption/degradation processes (Laffineur et al., 2011). Besides temperature, VPD and PAR modulate stomatal aperture and thus actively regulate the diffusion of methanol from the site of production to the atmosphere (Niinemets et al., 2004). Although we refrain from any further modelling of methanol flux due to the limited time resolution of our set of measurements, we suppose that in the long-term, deciduous forest such as poplar plantations may possibly act more as a sink than a source of methanol (Laffineur et al., 2011), based on the fact that periods of intense methanol production are limited to transient stages of leaf growth throughout the year, which may be even shortened by the frequent occurrence of adverse environmental condition of low temperature (characterizing Northern climates) or low soil moisture availability (in more Southern climates).

4.1.3. Other oxygenated-VOC

Besides isoprene and methanol emissions, we found deposition fluxes of formaldehyde to the vegetation (Fig. 3), most likely as a result of an increasing stomatal sink (Fig. 3) combined with a strengthening source (Fig. S3) developing throughout the day. Although formaldehyde has shown to be released from the vegetation only under extreme stress conditions (Fall et al., 2001; Brilli et al., 2012), in the atmosphere formaldehyde can be formed

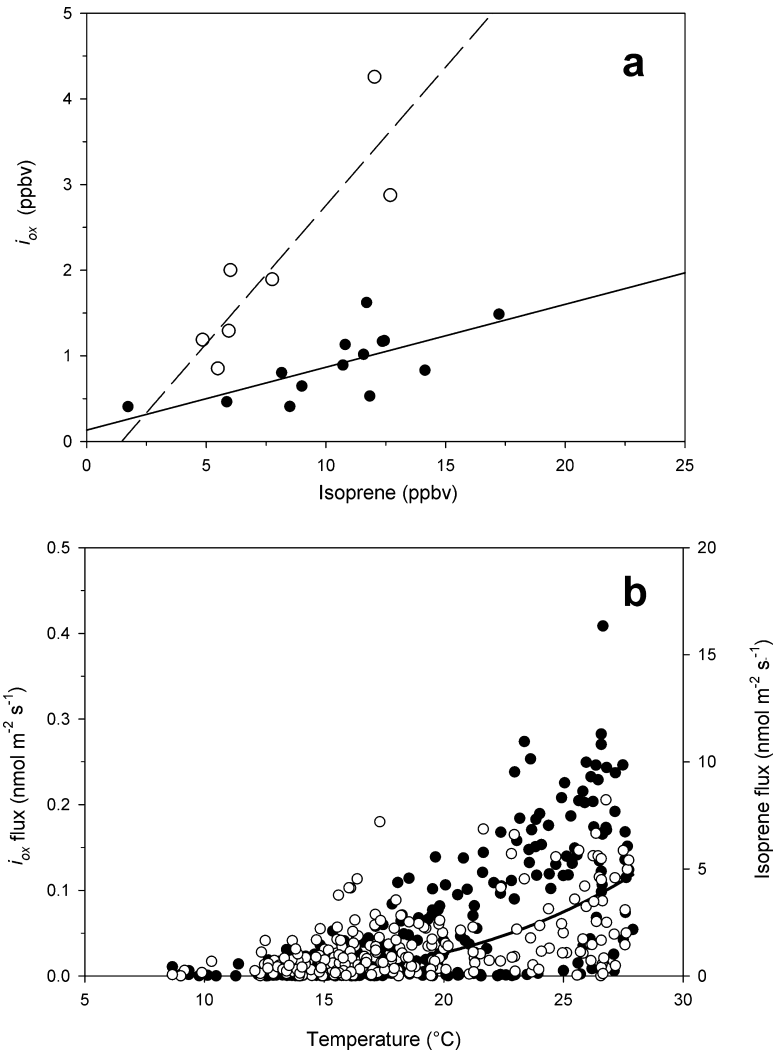

Fig. 7. Dependence of i_{ox} concentrations (ppbv) to isoprene concentrations (ppbv) measured (a) in 6 L samples of air exits the cuvette (set at 25 °C) enclosing a portion of poplar leaf and (closed circles) and in 6 L of ambient air sampled from the eddy covariance tower when the air temperature was around 25 ± 1 °C (open circles); (b) half-hourly eddy covariance fluxes of i_{ox} (open circles, left *y*-axis) and isoprene (closed circles, right *y*-axis) measured by PTR–TOF–MS during the whole period (16–28 July, 2012).

from isoprene under the presence of high NO_x concentrations (Millet et al., 2008). In fact the uptake of formaldehyde by the poplar plantation occurred particularly during the midday hours of the warming days, when high PAR and temperature coupled with increasing NO_x ambient concentrations (Fig. 1 f and g) stimulated at the same time isoprene production and the cycling of HO_x radicals.

Other oxygenated-VOC such as acetaldehyde, acetone and acetic acid were either emitted or deposited in the poplar plantation. In particular, deposition of oxygenated-VOC to the vegetation can be enhanced by the soil that has shown to behave as a sink more than as a source of VOC, although a tiny VOC exchange rate between the soil and the vegetation was measured (Asensio et al., 2007). However, the occurrence of low production by the vegetation, combined with rising ambient concentrations during the day (Karl et al., 2010; Langford et al., 2010; Misztal et al., 2011; Jardine et al., 2012), minimized the emission of these other oxygenated-VOC from the vegetation.

4.2. Fluxes at leaf-level

Our leaf-level measurements further confirmed the relationship between isoprene emission and leaf developmental stage (Fig. 6a) (Guidolotti et al., 2011). The magnitude of isoprene emission measured in adult leaves was similar among the poplar genotypes constituting the poplar plantation, which is in agreement with a previous study on *Populus spp.* (Guidolotti et al., 2011) confirming that isoprene emission rates are similar across *Populus spp*. Differently, juvenile poplar leaves belonging to different genotypes exhibited very low amounts of isoprene emissions, but were found to emit a quantitatively different blend of monoterpenes, although the compounds constituting the blend were always α- and β-pinene and (*E*)-β-ocimene. This confirmed a previous study conducted at another site and with a different poplar genotype (Brilli et al., 2009). Nevertheless, the emission of monoterpenes at ecosystem level was very tiny and often fell within the associated random uncertainty. These low emission rates could be due to the fact that monoterpene emission originates from only a small (apical) portion of the canopy (Brilli et al., 2009)

4.3 i_{ox} Fluxes at ecosystem- and leaf-level

One of the aims of this study was to quantify the importance of within-leaf isoprene oxidation. At ecosystem level, our analysis confirmed a strong positive correlation (R^2 = 0.78) between the concentrations of i_{ox} and isoprene in the atmosphere (Fig. 7a). The ratio between i_{ox}-to-isoprene fluxes depends on isoprene production

Table 3
Parameters are: R^2, correlation coefficient; a, b, c equation coefficients.

	Regression line	R^2	a	b	c	Standard error of estimate
Fig. 4a	$f = a\exp(bx)$	0.56*	0.01*	0.23**	–	$R^2 = 1.43$ $a = 3.7 \times 10^{-3}$ $b = 0.01$
Fig. 4b	$f = b + a\ln(\mathrm{abs}(x))$	0.65*	1.72**	−8.34**	–	$R^2 = 1.96$ $a = 0.12$ $b = 0.73$
Fig. 4c	$f = b + a\ln(\mathrm{abs}(x))$	0.39*	15.45**	−31.46**	–	$R^2 = 4.56$ $a = 2.29$ $b = 0.80$
Fig. 4d	$f = b + a\ln(\mathrm{abs}(x))$	0.58*	4.61**	0.21**	–	$R^2 = 3.78$ $a = 0.21$ $b = 1.27$
Fig. 5a	$f = c + a\exp(bx)$	0.68*	17.27	0.04	−25.66	$R^2 = 3.72$ $a = 58.77$ $b = 0.07$ $c = 58.78$
Fig. 5b	$f = c + a\exp(bx)$	0.49*	0.10	0.10**	−0.17	$R^2 = 0.24$ $a = 0.07$ $b = 0.03$ $c = 0.11$
Fig. 5c	$f = c + a\exp(bx)$	0.59*	1.95	0.07*	−3.43*	$R^2 = 1.77$ $a = 1.32$ $b = 0.02$ $c = 1.79$
Fig. 6a	$f = b + ax$	0.29*	1.58	0.79	–	–
Fig. 6b	$f = b + a\ln(\mathrm{abs}(x))$	0.40*	1.2**	−4.88**	–	$R^2 = 1.48$ $a = 0.09$ $b = 0.55$
Fig. 6c	$f = b + a\ln(\mathrm{abs}(x))$	0.25*	4.01**	−9.94**	–	$R^2 = 1.65$ $a = 0.32$ $b = 0.91$
Fig. 7a (cuvette)	$f = b + ax$	0.49*	0.073*	0.13	–	–
Fig. 7a (ambient air)	$f = b + ax$	0.78*	0.32*	−0.47	–	–
Fig. 7b	$f = c + a x\hat{}b$	0.33*	1.5×10^{-5}*	3.82**	–	$a = 2.1 \times 10^{-5}$* $b = 0.43$

One asterisk indicates significant with $p < 0.05$, and two asterisks indicate highly significant with $p < 0.001$.

rate and the concentration of $^{\bullet}$OH since i_{ox} are the major first-order products deriving from isoprene oxidation (Pierotti et al., 1990). Indeed isoprene oxidation in the atmosphere occurring during the day elevates the ambient concentration of i_{ox}. This can reach the compensation point, which in turn limits net i_{ox} emission by leaves. Detection of i_{ox} fluxes may have been complicated by the parallel occurrence of source (through isoprene oxidation processes) – and sink – (due to deposition) dynamics, also affecting the compensation point for i_{ox} (Karl et al., 2005; Tani et al., 2010). However, especially in the second, climatologically favourable measurement period, we measured net emission fluxes of i_{ox} also in the middle of the day, together with peak isoprene production, indicating that compensation point was not reached (Fig. 3). In our study, an average i_{ox}-to-isoprene ratio of 0.32 was observed when i_{ox} and isoprene were sampled in ambient air under a temperature of $25 \pm 1\,^{\circ}$C, similar to the ratios reported by Kesselmeier et al. (2002), Kuhn et al. (2007), Langford et al. (2010) and Misztal et al. (2011) across different ecosystems.

Also the leaf enclosure measurements using VOC-free air confirmed the emission of i_{ox} in *Populus* sp. (Jardine et al., 2012), which correlated directly with isoprene production ($R^2 = 0.49$) and showed a mean i_{ox}-to-isoprene concentration ratio of 0.073 (Fig. 7a). This ratio (=0.073) is lower than the one measured in ambient air (=0.32) under the same temperature. Therefore, about 20% of the i_{ox} that are found in the atmosphere could be formed by isoprene oxidation within poplar leaves. Moreover, it is likely that the fraction of within-plant i_{ox} production is in relation to active ROS formation, in turn enhanced by O_3 deposition entering leaves through stomata during the hot and sunny days in the last period of measurements (Fig. 3). I_{ox} could even proxy the amount of ozone that is scavenged by plants, if isoprene acts as the main sink of ozone within leaves (Loreto and Fares, 2007). The ability of poplars to use isoprene as a protective mechanism to tolerate oxidative stress (Vickers et al., 2009) may indicate their high tolerance to future scenarios where ozone concentrations are expected to increase, especially in NO_x-rich, industrialized areas (Lerdau, 2007).

5. Conclusion

In conclusion, this is one of the first studies reporting fluxes of both VOC and CO_2 at leaf- and at ecosystem-level in a poplar-based SRC plantation. Direct PTR–TOF–MS eddy covariance measurements confirmed abundant fluxes of isoprene from the plantation, but also revealed similarly high fluxes of methanol during a period of intensive growth. Detection of i_{ox} emission both with eddy covariance at ecosystem-level and with enclosure measurements at leaf-level confirmed that a fraction of the produced isoprene is oxidized before being emitted in the atmosphere, especially when plants produce ROS or take up ozone during warm and sunny days.

Acknowledgments

This study was financially supported by the European Commission's Seventh Framework Programme (FP7/2007-2013) as a European Research Council Advanced Grant (no. 233366, POPFULL) as well as by the Flemish Hercules Foundation as Infrastructure contract ZW09-06. Joris Cools is greatly acknowledged for his help with set-up installation and maintenance. We also thank Alessandro Zaldei for his contribution during the set-up installation and Eugen Hartungen for PTR–TOF–MS assistance during the field campaign.

Appendix A. Supplementary data

Supplementary data associated with this article can be found, in the online version, at http://dx.doi.org/10.1016/j.agrformet.2013.11.006.

References

Asensio, D., Peñuelas, J., Filella, I., Llusià, J., 2007. On-line screening of soil VOCs exchange responses to moisture, temperature and root presence. Plant Soil 291, 249–261.

Ashworth, K., Wild, O., Hewitt, C.N., 2013. Impacts of biofuel cultivation on mortality and crop yields. Nat. Clim. Change, http://dx.doi.org/10.1038/NCLIMATE1788.

Atkinson, R., Arey, J., 2003. Atmospheric degradation of volatile organic compounds. Chem. Rev. 103, 4605–4638.

Aubinet, M., Grelle, A., Ibrom, A., Rannik, Ü., Moncrieff, J., Foken, T., Kowalski, A.S., Martin, P.H., Berbigier, P., Bernhofer, C., Clement, R., Elbers, J., Granier, A., Gŕunwald, T., Morgenstern, K., Pilegaard, K., Rebmann, C., Snijders, W., Valentini, R., Vesala, T., 2000. Estimates of the annual net carbon and water exchange of forests: the EUROFLUX methodology. Adv. Ecol. Res. 30, 113–175.

Brilli, F., Hörtnagl, L., Bamberger, I., Schnitzhofer, R., Ruuskanen, T.M., Hansel, A., Loreto, F., Wohlfahrt, G., 2012. Qualitative and quantitative characterization of volatile organic compound emissions from cut grass. Environ. Sci. Techol. 46, 3859–3865.

Brilli, F., Ciccioli, P., Frattoni, M., Prestininzi, M., Spanedda, A.F., Loreto, F., 2009. Constitutive and herbivore-induced monoterpenes emitted by *Populus* × *euroamericana* leaves are key volatiles that orient *Chrysomela populi* beetles. Plant Cell Environ. 32, 542–552.

Brilli, F., Barta, C., Fortunati, A., Lerdau, M., Loreto, F., Centritto, M., 2007. Response of isoprene emission and carbon metabolism to drought in white poplar (*Populus alba*) saplings. New Phytol. 175, 244–254.

Broeckx, L.S., Verlinden, M.S., Vangronsveld, J., Ceulemans, R., 2012. Importance of crown architecture for leaf area index of different *Populus* genotypes in a high-density plantation. Tree Physiol. 32, 1214–1226.

Cai, T.B., Price, D.T., Orchansky, A.L., Thomas, B.R., 2011. Carbon, water, and energy exchanges of a hybrid poplar plantation during the first five years following planting. Ecosystems 14, 658–671.

Chameides, W.L., Lindsay, R.W., Richardson, J., Kiang, C.S., 1988. The role of biogenic hydrocarbons in urban photochemical smog: Atlanta as a case study. Science 241, 1473–1475.

Claeys, M., Graham, B., Vas, G., Wang, W., Vermeylen, R., Pashynska, Cafmeyer, J., Guyon, P., Andreae, M.O., Artaxo, P., Maenhaut, W., 2013. Formation of secondary organic aerosols through photooxidation of isoprene. Science 303, 1173–1176.

Calfapietra, C., Gielen, B., Karnosky, D., Ceulemans, R., Scarascia-Mugnozza, S., 2010. Response and potential of agroforestry crops under global change. Environ. Pollut. 158, 1095–1104.

EU, 2009. In: Union OjotE (Ed.), Directives 2001/77/EC and 2003/30/EC. O. J. o. t. E. Union. EU, Brussels, Directive 2009/28/EC of the European Parliament and of the Council of 23 April 2009 on the promotion of the use of energy from renewable sources and amending and subsequently repealing.

Fall, R., Karl, T., Jordan, A., Lindinger, W., 2001. Biogenic C5VOCs: release from leaves after freeze-thaw wounding and occurrence in air at a high mountain observatory. Atm. Environ. 35, 3905–3916.

Farmer, E.E., 2001. Surface-to-air signals. Nature 411, 854–856.

Fares, S., Park, J.H., Gentner, D.R., Weber, R., Ormeño, E., Karlik, J., Goldstein, A.H., 2012. Seasonal cycles of biogenic volatile organic compound fluxes and concentrations in a California citrus orchard. Atmos. Chem. Phys. 12, 9865–9880.

Fargione, J., Hill, J., Tilman, D., Polasky, S., Hawthorne, P., 2008. Land clearing and the biofuel carbon debt. Science 319, 1235–1238.

Finkelstein, P.L., Sims, P.F., 2001. Sampling error in eddy correlation flux measurements. J. Geophys. Res. 27, 3503–3509.

Fisher, G., Prieler, S., van Velthuizen, H., Berndes, G., Faaij, A., Londo, M., de Wit, M., 2010. Biofuel production potentials in Europe: sustainableuse of cultivated land and pastures. Part II: Land use scenarios. Biomass and Bioenergy 34, 173–187.

Folkers, A., Hüve, K., Ammann, C., Dindorf, T., Kesselmeier, J., Kleist, E., Kuhn, U., Uerlings, R., Wildt, J., 2008. Methanol emissions from deciduous tree species: dependence on temperature and light intensity. Plant Biol. 10, 65–75.

Fortunati, A., Barta, C., Brilli, F., Centritto, M., Zimmer, I., Schnitzler, J.P., Loreto, F., 2008. Isoprene emission is not temperature-dependent during and after severe drought-stress: a physiological and biochemical analysis. Plant J. 55, 687–697.

Fratini, G., Ibrom, A., Arriga, N., Burba, G., Papale, D., 2012. Relative humidity effects on water vapour fluxes measured with closed-path eddy-covariance systems with short sampling lines. Agric. For. Meteorol. 147, 209–232.

Frenkel, C., Peters, J.S., Tieman, D.M., Tiznado, M.E., Handa, A.K., 1998. Pectin methylesterase regulates methanol and ethanol accumulation in ripening tomato (*Lycopersicon esculentum*) fruit. J. Biol. Chem. 273, 4293–4295.

Fuentes, J.D., Wang, D., Gu, L., 1999. Seasonal variations in isoprene emissions from a boreal aspen forest. J. Appl. Meteorol. 38, 855–869.

Gaffe, J., Tuieman, D.M., Handa, A.K., 1994. Pectin methylesterase isoforms in tomato (Lycopersicon esculentum) tissues. Effects of expression of a pectin methylesterase antisense gene. Plant Physiol. 105, 199–203.

Göckede, M., Rebmann, C., Foken, T., 2004. A combination of quality assessment tools for eddy covariance measurements with footprint modelling for the characterisation of complex sites. Agric. For. Meteorol. 127, 175–188.

Graus, M., Müller, M., Hansel, A., 2010. High resolution PTR–TOF quantification and formula confirmation of VOC in real time. J. Am. Soc. Mass Spectrom. 21, 1037–1044.

Guenther, A., Zimmerman, P., Harley, P., Monson, R., Fall, R., 1993. Isoprene and monoterpene emission rate variability: model evaluation and sensitivity analysis. J. Geophys. Res. 98, 12609–12617.

Guidolotti, G., Calfapietra, C., Loreto, F., 2011. The relationship between isoprene emission, CO_2 assimilation and water use efficiency across a range of poplar genotypes. Physiol. Plant 142, 297–304.

Hakola, H., Rinne, J., Laurila, T., 1998. The hydrocarbon emission rates of tea-leafed willow (*Salix phylicipolia*), silver birch (*Betula pendula*) and European aspen (*Populus tremula*). Atmos. Environ. 32, 1825–1833.

Horst, T.W., Lenschow, D.H., 2009. Attenuation of scalar fluxes measured with spatially-displaced sensors. BoundaryLayer Meteorol. 130, 275–300.

Hörtnagl, L., Bamberger, I., Graus, M., Ruuskanen, T.M., Schnitzhofer, R., Müller, M., Hansel, A., Wohlfahrt, G., 2011. Biotic, abiotic, and management controls on methanol exchange above a temperate mountain grassland. J. Geophys. Res. 116, G03021.

Hüve, K., Christ, M.M., Kleist, E., Uerlings, R., Niinemets, U., Walter, A., Wildt, J., 2007. Simultaneous growth and emission measurements demonstrate an interactive control of methanol release by leaf expansion and stomata. J. Exp. Bot. 58, 1783–1793.

Ibrom, A., Dellwik, E., Flyvbjerg, H., Jensen, N.O., Pilegaard, K., 2007. Strong low-pass filtering effects on water vapour flux measurements with closed-path eddy correlation systems. Agric. For. Meteorol. 147, 140–156.

International Poplar Commission (IPC), 24th Session and 46th Executive Committee Meeting, 2013. http://www.fao.org/forestry/ipc2012/en/

Jardine, K.J., Monson, R.K., Abrell, L., Saleska, S.R., Arneth, A., Jardine, A., Ishida, F.Y., Serrano, A.M.Y., Artaxo, P., Karl, T., Fares, S., Goldstein, A., Loreto, F., Huxman, T., 2012. Within-plant isoprene oxidation confirmed by direct emission of oxidation products methyl vinyl ketone and methacrolein. Global Change Biol. 18, 973–984.

Jordan, A., Haidacher, S., Hanel, G., Hartungen, E., Märk, L., Seehauser, H., Schottkowsky, R., Sulzer, P., Märk, T.D., 2009. A high resolution and high sensitivity proton-transfer-reaction time-of-flight mass spectrometer (PTR–TOF–MS). Int. J. Mass Spectrom. 286, 122–128.

Karl, T., Harley, P., Emmons, L., Thornton, B., Guenther, A., Basu, C., Turnipseed, A., Jardine, K., 2010. Efficient atmospheric cleansing of oxidized organic trace gases by vegetation. Science 330, 816–819.

Karl, T., Guenther, A., Turnipseed, A., Tyndall1, G., Artaxo, P., Martin, S., 2005. Rapid formation of isoprene photo-oxidation products observed in Amazonia. Atmos. Chem. Phys. 9, 7753–7767.

Kesselmeier, J., Kuhn, U., Rottenberger, S., Biesenthal, T., Wolf, A., Schebeske, G., Andreae, M.O., Ciccioli, P., Brancaleoni, E., Frattoni, M., Oliva, S.T., Botelho, M.L., Silva, C.M.A., Tavares, T.M., 2002. Concentrations and species composition of atmospheric volatile organic compounds (VOCs) as observed during the wet and dry season in Rondonia (Amazonia). J. Geophys. Res. Atmos. 107 (D20), 8053.

Kesselmeier, J., Staudt, M., 1999. Biogenic volatile compounds (VOC): an overview on emission, physiology and ecology. J. Atmos. Chem. 33, 23–88.

Kiendler-Scharr, A., Wildt, J., Dal Maso, M., Hohaus, T., Kleist, E., Mentel, T.F., Tillmann, R., Uerlings, R., Schurr, U., Wahner, A., 2009. New particle formation in forest inhibited by isoprene emission. Nature 461, 381–384.

Kuhn, U., Andreae, M.O., Ammann, C., Araüjo, A.C., Brancaleoni, E., Ciccioli, P., Dindorf, T., Frattoni, M., Gatti, L.V., Ganzeveld, L., Kruijt, B., Lelieveld, J., Lloyd, J., Meixner, F.X., Nobre, A.D., Pöschl, U., Spirig, C., Stefani, P., Thielmann, A., Valentini, R., Kesselmeier, J., 2007. Isoprene and monoterpene fluxes from Central Amazonian rainforest inferred from towerbased and airborne measurements, and implications on the atmospheric chemistry and the local carbon budget. Atmos. Chem. Phys. 7, 2855–2879.

Kulmala, M., Hameri, K., Aalto, P.O., Makela, J.M., Pirjola, L., Nilsson, E.D., Buzorius, G., Rannik, U., Dal Maso, M., Seidl Hoffman, T., Janson, R., Hansson, H.C., Viisanen, Y., Laaksonen, A., O'Dowd, C.D., 2001. Overview of the international project on biogenic aerosol formation in the boreal forest (BIOFOR). Tellus 53, 324–343.

Laffineur, Q., Aubinet, M., Schoon, N., Amelynck, C., Müller, J.-F., Dewulf, J., Van Langenhove, H., Steppe, K., Heinesch, B., 2011. Abiotic and biotic control of methanol exchanges in a temperate mixed forest. Atmos. Chem. Phys. 12, 577–590.

Langford, B., Misztal, P.K., Nemitz, E., Davison, B., Helfter, C., Pugh, T.A.M., MacKenzie, A.R., Lim, S.F., Hewitt, S.F.C.N., 2010. Fluxes and concentrations of volatile organic compounds from a south-east Asian tropical rainforest. Atmos. Chem. Phys. 10, 8391–8412.

Laothawornkitkul, J., Paul, N.D., Vickers, C.E., Possel, M., Taylor, J.E., Mullineaux, P.M., Hewitt, C.N., 2008. Isoprene emissions influence herbivore feeding decisions. Plant Cell Environ. 31, 1410–1415.

Lerdau, M., 2007. A positive feedback with negative consequences. Science 316, 212–213.

Loivamaäki, M., Mumm, R., Dicke, M., Schnitzler, J.-P., 2008. Isoprene interferes with the attraction of bodyguards by herbaceous plants. PNAS 105, 17430–17435.

Loreto, F.J.P., Schnitzler, 2010. Abiotic stresses and induced BVOCs. Trends Plant Sci. 15, 154–166.

Loreto, F., Fares, S., 2007. Is ozone flux inside leaves only a damage indicator? Clues from volatile isoprenoid studies. Plant Physiol. 143, 1096–1100.

Loreto, F., Velikova, V., 2001. Isoprene produced by leaves protects the photosynthetic apparatus against ozone damage, quenches ozone products, and reduces lipid peroxidation of cellular membranes. Plant Physiol. 127, 1781–1787.

Loreto, F., Sharkey, T., 1990. A gas-exchange study of photosynthesisand isoprene emission in *Quercus rubra* L. Planta 182, 523–531.

Lloyd, J., Taylor, J.A., 1994. On the temperature dependence of soil respiration. Funct. Ecol. 8, 315–323.
Mayrhofer, S., Teuber, M., Zimmer, I., Louis, S., Fischbach, R.J., Schnitzler, P.J., 2005. Diurnal and seasonal variation of isoprene biosynthesis-related genes in grey poplar leaves. Plant Physiol. 139, 474–484.
Migliavacca, M., Meroni, M., Manca, G., Matteucci, G., Montagnani, L., Grassi, G., Zenone, T., Teobaldelli, M., Goded, I., Colombo, R., Seufert, G., 2009. Seasonal and interannual patterns of carbon and water fluxes of a poplar plantation under peculiar eco-climatic conditions. Agric. For. Meteorol. 147, 209–232.
Millet, D.B., Jacob, D.J., Boersma, K.F., Fu, T.M., Kurosu, T.P., Chance, K., Heald, C.L., Guenther, A., 2008. Spatial distribution of isoprene emissions from North America derived from formaldehyde column measurements by the OMI satellite sensor. J. Geophys. Res. Atmos. 113, D02307, http://dx.doi.org/10.1029/2007jd008950.
Misztal, P.K., Nemitz, E., Langford, B., Di Marco, C.F., Phillips, G.J., Hewitt, C.N., MacKenzie, A.R., Owen, S.N., Fowler, D., Heal, M.R., Cape, J.N., 2011. Direct ecosystem fluxes of volatile organic compounds from oil palms in south-east Asia. Atmos. Chem. Phys. 11, 8995–9017.
Moffat, A.M., Papale, D., Reichstein, M., Hollinger, D.Y., Richardson, A.D., Barr, A.G., Beckstein, C., Braswell, B.H., Churkina, G., Desai, A.R., Falge, E., Gove, J.H., Heimann, M., Hui, D., Jarvis, A.J., Kattge, J., Noormets, A., Stauch, V.J., 2007. Comprehensive comparison of gap-filling techniques for eddy covariance net carbon fluxes. Agric. For. Meteorol. 147, 209–232.
Moncrieff, J., Clement, R., Finnigan, J., Meyers, T., 2004. In: Lee, X., Massman, W., Law, B. (Eds.), Handbook of Micrometeorology: A Guide for Surface Flux Measurement and Analysis. Kluwer Academic Publisher, Dordrecht, pp. 7–32.
Moncrieff, J.B., Massheder, J.M., deBruin, H., Elbers, J., Friborg, T., Heusinkveld, B., Kabat, P., Scott, S., Soegaard, H., Verhoef, A., 1997. A system to measure surface fluxes of momentum, sensible heat, water vapour and carbon dioxide. J. Hydrol. 189, 589–611.
Monson, R.K., Jaeger, C.H., Adams III, W.W., Driggers, E.M., Silver, G.M., Fall, R., 1992. Relationships among isoprene emission rate, photosynthesis, and isoprene synthase activity as influenced by temperature. Plant Physiol. 98, 1175–1180.
Müller, M., Graus, M., Ruuskanen, T.M., Schnitzhofer, R., Bamberger, I., Kaser, L., Titzmann, T., Hörtnagl, L., Wohlfahrt, G., Karl, T., Hansel, A., 2010. First eddy covariance flux measurements by PTR–TOF. Atmos. Meas. Tech. 3, 387–395.
Müller, M., Mikoviny, T., Jud, W., D'Anna, B., Wisthaler, A., 2013. A new software tool for the analysis of high resolution PTR–TOF mass spectra. Chemom. Intell. Lab. Syst. 127, 158–165.
Nemecek-Marshall, M., Macdonald, R.C., Franzen, F.J., Wojciechowski, C.L., Fall, R., 1995. Methanol emission from leaves–enzymatic detection of gas-phase methanol and relation of methanol fluxes to stomatal conductance and leaf development. Plant Physiol. 108, 1359–1368.
Niinemets, Ü., Loreto, F., Reichstein, M., 2004. Physiological and physicochemical controls on foliar volatile organic compound emissions. Trends Plant Sci. 9, 180–186.
Niinemets, Ü., Reichstein, M., 2003. Controls on the emission of plant volatiles through stomata: differential sensitivity of emission rates to stomatal closure explained. J. Geophys. Res. 108, 4208.
Oikawa, P.Y., Giebel, B.M., Sternberg, D.L.D.O., Li, L., Timko, M.P., Swart, P.K., Riemer, D.D., Mak, J.E., Lerdau, M.T., 2011. Leaf and root pectin methylesterase activity and C-13/C-12 stable isotopic ratio measurements of methanol emissions give insight into methanol production in Lycopersicon esculentum. New Phytol. 191, 1031–1040.
Özdemir, E.D., Härdtlein, M., Eltrop, L., 2009. Land substitution effects of biofuel side products and implications on the land area requirement for EU 2020 biofuel targets. Energy Policy 37, 2986–2996.
Papale, D., Reichstein, M., Aubinet, M., Canfora, E., Bernhofer, C., Kutsch, W., Longdoz, B., Rambal, S., Valentini, R., Vesala, T., Yakir, D., 2006. Towards a standardized processing of Net Ecosystem Exchange measured with eddy covariance technique: algorithms and uncertainty estimation. Biogeosciences 3, 571–583.
Pierotti, D., Wofsy, S.C., Jacob, D., Rasmussen, R.A., 1990. Isoprene and its oxidation-products—methacrolein and methyl vinyl ketone. J. Geophys. Res. Atmos. 95, 1871–1881.
Pinho, P.G., Pio, C.A., Jenkin, M.E., 2005. Evaluation of isoprene degradation in the detailed tropospheric chemical mechanism, MCM v3, using environmental chamber data. Atmos. Environ. 39, 130–1322.
Rannik, Ü., Vesala, T., 1999. Autoregressive filtering versus linear detrending in estimation of fluxes by the eddy covariance method. BoundaryLayer Meteorol. 91, 259–280.
Reichstein, M., Falge, E., Baldocchi, D., Papale, D., Aubinet, M., Berbigier, P., Bernhofer, C., Buchmann, N., Gilmanov, T., Granier, A., Grunwald, T., Havrankova, K., Ilvesniemi, H., Janous, D., Knohl, A., Laurila, T., Lohila, A., Loustau, D., Matteucci, G., Meyers, T., Miglietta, F., Ourcival, J.-M., Pumpanen, J., Rambal, S., Rotenberg, E., Sanz, M., Tenhunen, J., Seufert, G., Vaccari, F., Vesala, T., Yakir, D., Valentini, R., 2005. On the separation of net ecosystem exchange into assimilation and ecosystem respiration: review and improved algorithm. Global Change Biol. Bioenergy 11 (9), 1424–1439.
Ruuskanen, T.M., Müller, M., Schnitzhofer, R., Karl, T., Graus, M., Bamberger, I., Hörtnagl, L., Brilli, F., Wohlfahrt, G., Hansel, A., 2011. Eddy covariance VOC emission and deposition fluxes above grassland using PTR–TOF. Atmos. Chem. Phys. 11, 611–625.
Searchinger, T., Heimlich, R., Houghton, R.A., Dong, F., Elobeid, A., Fabiosa, J., Tokgoz, S., Hayes, D., Yu, T.H., 2008. Use of U.S. cropland for biofuels increases greenhouse gasses through emissions from land-use change. Science 319, 1238–1240.
Sharkey., T.D., Wiberley, A.E., Donohue, A.R., 2008. Isoprene emission from plants: why and how. Ann. Bot. 101, 5–18.
Sharkey, T.D., Yeh, S., 2001. Isoprene emission from plants. Annu. Rev. Plant Biol. 52, 407–436.
Staudt, M., Lhoutellier, L., 2011. Monoterpene and sesquiterpene emissions from *Quercus coccifera* exhibit interacting responses to light and temperature. Biogeosciences 8, 2757–2771.
Tani, A., Tobe, S., Shimizu, S., 2010. Uptake of methacrolein and methyl vinyl ketone by tree saplings and implications for forest atmosphere. Environ. Sci. Technol. 44, 7096–7101.
U.S., 2011. Renewable Fuel Standard RFS. Environmental Protection Agency, EPA, Washington, DC http://www.epa.gov/otaq/fuels/renewablefuels/index.htm
Velikova, V., La Mantia, T., Lauteri, M., Michelozzi, M., Nogues, I., Loreto, F., 2012. The impact of winter flooding with saline water on foliar carbon uptake and the volatile fraction of leaves and fruits of lemon (Citrus × limon) trees. Funct. Plant Biol. 39, 199–213.
Velikova, V., Pinelli, P., Pasqualini, S., Reale, L., Ferranti, F., Loreto, F., 2005. Isoprene decreases the concentration of nitric oxide in leaves exposed to elevated ozone. New Phytol. 166, 419–426.
Vickers, C.E., Gershenzon, J., Lerdau, M.T., Loreto, F., 2009. A unified mechanism of action for volatile isoprenoids in plant abiotic stress. Nat. Chem. Ecol. 5, 283–291.
Vitousek, P.M., 1991. Can planted forests counteract increasing atmospheric carbon dioxide? J. Environ. Qual. 20, 348–354.
Weih, M., 2004. Intensive short rotation forestry in boreal climates: present and future perspectives. Can. J. For. Res. 34, 1369–1378.
Wiberley, A.E., Linskey, A.R., Falbel, T.G., Sharkey, T.D., 2005. Development of the capacity for isoprene emission in kudzu. Plant Cell Environ. 28, 898–905.
Wilczak, J.M., Oncley, S.P., Stage, S.A., 2001. Sonic anemometer tilt correction algorithms. Boundary-Layer Meteorol. 99, 127–150.
Zona, D., Janssens, I., Gioli, B., Jungkunst, E.F., Serrano, M.C., Ceulemans, R., 2012. N_2O fluxes of a bio-energy poplar plantation during a two years rotation period. Global Change Biol. Bioenergy, http://dx.doi.org/10.1111/gcbb.12019.
Zona, D., Janssens, I., Aubinet, M., Gioli, B., Vicca, S., Fichot, R., Ceulemans, R., 2013. Fluxes of the greenhouse gases (CO_2, CH_4 and N_2O) above a short-rotation poplar plantation after conversion from agricultural land. Agric. For. Metereol. 169, 100–110.
Zona, D., Gioli, B., Fares, S., De Groote, T., Pilegaard, K., Ibrom, A., Ceulemans, R., 2014. Environmental controls on ozone fluxes in a poplar plantation in western Europe. Environ. Poll. 184, 201–210.